Joint Institute for Nuclear Research

ANNUAL REPORT

on results of the development
of the NICA accelerator block in 2021 - 2022

as of 01/12/2022

Dubna, 2022

Contents:

1. Introduction

This document briefly describes general works performed in the frame of the NICA accelerator complex development from October 2021 to date.

The main directions of the works were as follows:

- Commissioning of the accelerator complex elements (ion sources, HILAC, Booster, Nuclotron, beam transport lines) with ion beams during dedicated runs.
- Development of experimental zones for the NICA innovation program.
- Assembly of the NICA collider and preparation for its commissioning.

More detailed information about systems under development is presented in the dedicated addendums. Main results of the works as well as the status of the project were presented at accelerator conferences and published in scientific journals.

List of the addendums:

Addendum #1. Elements of the injection complex, SOCHI station

Addendum #2. Booster synchrotron, results of the first runs

Addendum #3. Beam transport from the Booster into the Nuclotron

Addendum #4. Beam transfer channel to the experimental set-ups in Building 205 and to the Measurement Pavilion

2. Period between the second and third runs (October-December 2021)

After the beam was successfully transported through the Booster–Nuclotron beam transfer line during the second commissioning, the next steps in the accelerator facility commissioning were the test of a stripping target at extraction from the Booster, realization of the beam injection into the Nuclotron, the beam acceleration, extraction and transportation to the experimental facilities.

The Nuclotron single turn beam injection system allows placing a bunch transported from the Booster into the equilibrium orbit of the Nuclotron. The system consists of a Lambertson magnet displacing the beam to the orbit plane and a pulsed ironless dipole magnet – the kicker compensating the angle between injected beam and the orbit. Both devices were assembled, tested and installed at the Nuclotron during preparation to the third commissioning run. More detailed description is presented in Addendum #3.

The Lambertson magnet (Fig. 1) is a dipole magnet with two apertures: the separated areas for the injected and circulating beams. In the first area, a horizontal magnetic field of up to 1.1 T is initiated by superconducting windings that deflect the injected beam vertically. Both areas are separated by a steel wall of special form to minimize the scattered magnetic field in the circulation region. Even more, to decrease the level of this scattered field, a superconducting coil compensating this field is placed. The Lambertson magnet and the compensating coil are powered from individual power supplies.

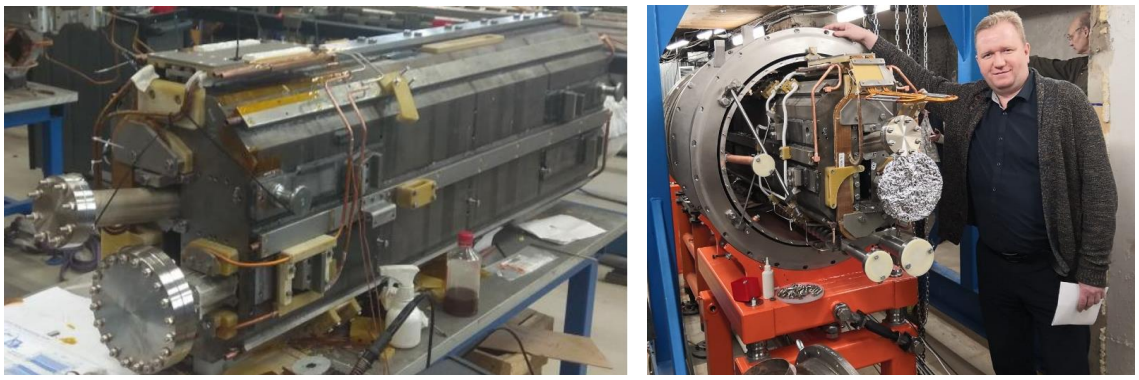

Fig. 1. Assembling of the Lambertson magnet (left) and installation at the Nuclotron (right).

The walls of the vacuum chamber somewhat reduce the acceptance of the Nuclotron. To restore it to the initial value during beam injection, the exit of the Lambertson magnet was shifted by 15 mm.

The kicker of 2 m length (Fig.2) consists of two pairs of conductors installed inside a vacuum box. Conductors are switched so that they form a magnetic field perpendicular to the plane of the beam orbit. The injection kicker pulse is synchronized with the Booster extraction one with account to the bunch time of flight through the transport line.

Fig.2 Nuclotron injection kicker: design of the electrodes (upper photo), assembly in the vacuum chamber (bottom photo).

During the previous commissioning runs, the cooling of the Booster's cryo-magnetic system was provided by temporary scheme. In order to provide the simultaneous cooling of the two rings, the cryogenic transport lines were reassembled for cooling of the Booster using satellite refrigerator (Fig. 3), mounted in 2021.

Fig. 3. Satellite refrigerator RSH-2000/4.5.

The stable operation of the compressor equipment was ensured by putting into operation a constant volume helium gasholder (Fig. 4).

Fig. 4. Helium gasholder of 1000 m^3.

The assembly of the SOCHI station of the NICA innovation block (dedicated to test microchips at 3.2 MeV/u energy) was started in October 2021.

The description of the beam transfer line from HILAC to SOCHI and details about SOCHI design are presented in Addendum #1.

Integration of the SOCHI station at a pressure of 10^{-3} Pa into the HILAc-Booster channel at a pressure of 10^{-6} Pa requires the following vacuum equipment: a cryogenic trap, pulsed diaphragm and turbomolecular pumps. This equipment should prevent the ingress of heavy gases into the existing HILAc-Booster transfer line and in the Booster, where the pressure is 10^{-9} Pa. According to the results of the vacuum tests in November-December 2021, it was confirmed that the developed and manufactured vacuum system of the SOCHI station and beam transfer line meet these requirements.

The particle collimation system (CS) is designed to reduce the beam current from a mA level in the HILAc to the hundred nA level required for chip irradiation. The CS is installed in the existing HILAc-Booster channel in front of a triplet of quadrupole lenses. It includes: a 50 μm stainless foil target unit with several slits - 260 μm×35 mm, 30 μm×35 mm, and 234 holes 30×15 μm with a step of 150 μm; a movement system VAb Vacuum-Anlagenbau GmbH (model MSI 40-100 S2, the positioning accuracy of ±100 μm controlled by a linear potentiometer, way of movement is 100 mm); vacuum fittings.

The SOCHI station (Fig. 5) includes:

- a vacuum chamber,
- pumping equipment,
- a gas composition analyzer and pressure control;
- a positioning and movement system for the test board with device under test (DUT), including a laser guidance system;
- a universal test board for DUT;
- a temperature setting system;
- a beam diagnostics and control system, including a positioning and movement system for detectors of the beam diagnostics and control system;
- a control panel;
- workplaces in the control room and experimental hall.

Inside the SOCHI vacuum chamber there are a positioning system for DUT, universal test board for connecting the test equipment with DUT, DUT itself, cables, a heating module, a phosphor detector of full absorption and a gas analyzer.

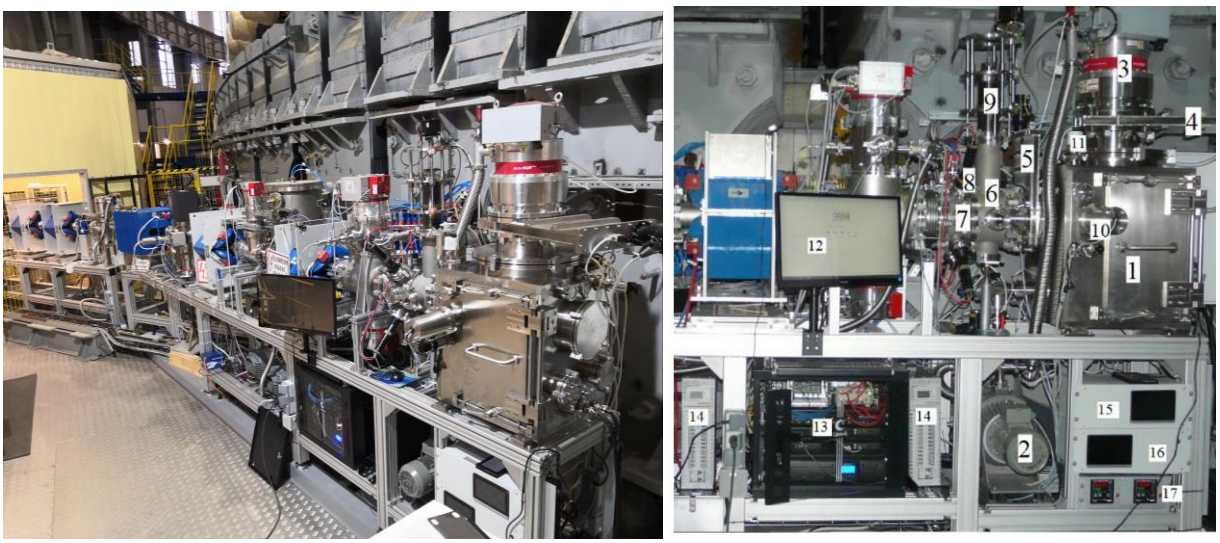

Fig. 5: External view of the SOCHI station with the main components: 1 – main vacuum chamber; 2 – forevacuum pump; 3 – turbo molecular pump; 4 – gate valve; 5 – gate valve; 6 – vacuum chamber 2; 7 – vacuum chamber 1; 8 – real-time beam parameter monitoring system; 9 – detector positioning system; 10 – video monitoring system for positioning DUT; 11 – vacuum gauge; 12 – monitor of the control panel; 13 – rack with control equipment; 14 – voltage stabilizer; 15 – vacuum system control unit; 16 – control unit of the DUT positioning system; 17 – temperature setting system control units.

The SOCHI station was mounted in December 2021. The physical start-up of the station was provided during the tuning of the LIS and HILAC for C^{4+} beam generation and acceleration [1]. The ion beam current at the exit of the HILAC in front of the CS was 3.5 mA, pulse duration - 3 μs, repetition period - 4 s. The photo in Fig. 6 shows the beam spot on the phosphor detector. The shadows of the system for online diagnostics and control of peripheral ion flux density and fluence (four scintillators) are seen in the corners.

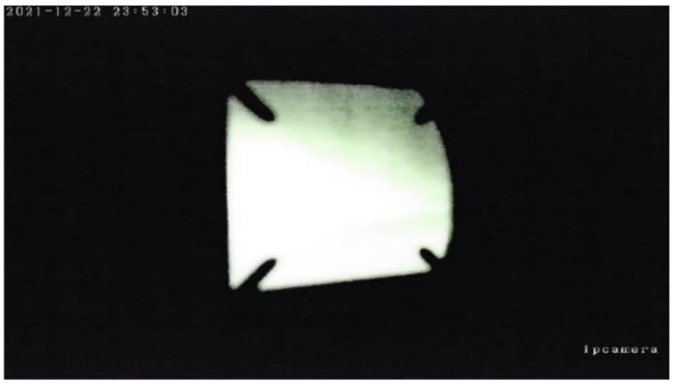

Fig.6: Internal view of the SOCHI vacuum chamber.

The maximum rate of the pulse radiation dose on the silicon semiconductor should be less than 1 rad/μs. To provide this radiation dose rate, a collimator with 20 holes 30 μm in diameter with a step of 700 μm between them to reduce beam current on target to the level of few hundreds of nA was used.

To the start of the run, the assembly and test of a new power supply system of magnetic elements in the extracted beam lines were completed (Fig. 7). The main features of the power supply system are high indicators for the accuracy of maintaining high current values (current from 600 to 4000 A) at relatively low voltage values (from 75 to 230 V DC). The power supply system has redundancy on the supply voltage side and on the DC side.

The system comprises the following elements:

- 6 kV network switchgear (SG) substation No. 15;
- power transformers 6/0.69kV;
- a 0.69 kV network switch gear;
- high precision power supplies;
- switching cabinets;
- cable communications;
- an automated control system.

The connection of the projected power supply system to the power grids of JINR provided at the voltage level of 6 kV to five cells of outgoing lines of reconstructed substation No. 15. The rated power of the power supply system is accepted in the amount of up to 5000 kVA.

The details of the extracted beam lines and the power supply system are presented in Addendum #4.

Fig. 7. Installation of the power supply units.

All the arc's dipole magnets of the collider were assembled and tested in 2021 [2]. Their installation into the tunnel started in December 2021 (Fig. 8).

Fig. 8. 28 December, 2021. Installation of the first collider dipole magnet in the tunnel

3. The third commissioning run

The initial period of the run (started on January 2) was dedicated to the optimization of cryo-cooling of the Booster and Nuclotron. For the first time the satellite refrigerator was used for the Booster cooling. The Booster cooldown time was about two times longer than the calculated one (7 days) due to unpredicted parasitic heat exchange between direct and back helium flows in the separators.

The cold mass of the Lambertson magnet installed at the right half-ring of the Nuclotron is substantialy larger than all other magnets and the cooling dynamics was dominated by this fact.

During the run, the accelerator complex was used for acceleration of the carbon ions generated by a laser ion source (LIS, Addendum #1). LIS and HILAC were tuned for C^{4+} as a compromise between the beam intensity and stable operation of the HILAC (designed for acceleration of the ions at the mass-to-charge ratio of 6).

Tuning of the Booster cycle included the adiabatic capture at injection (at the 5^{th} harmonics), recapture at 65 MeV/u (at the 1^{st} harmonics), acceleration up to the energy of 263 MeV/n and fast single-turn extraction, and it was provided as in the previous runs (see Addendum #2, [3]). The intensity of the accelerated beam reached about 3×10^9 particles, that is sufficient for all goals of the run.

The first circulation of the beam in the Booster was achieved without activation of the orbit correction system (Addendum #2). However, for the stable beam acceleration, optimization of the orbit bump during the beam extraction, the dynamic orbit correction is necessary. Moreover, an experience of the orbit correction is of great importance for the future collider operation. In the course of preparation for the Booster orbit correction the following works were performed:

- debugging of the corrector power supplies,
- debugging of the corrector power supplies software,
- development of the Tango-device for reading and storage of data from 24 BPMs in each plane,
- storage of the Beam Position Monitors (BPM) data each 100 ms,
- development of the Tango-device for measuring differential orbits in the automatic mode.

The measurements of the differential orbits and the closed orbit response matrix were performed (Fig. 9).

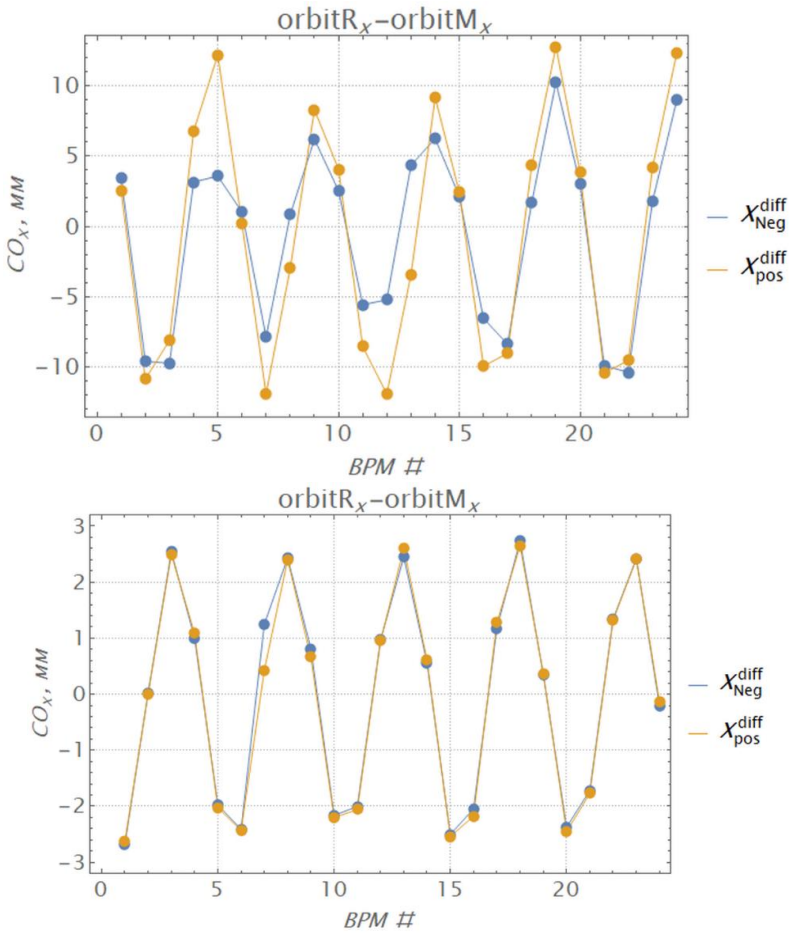

Fig. 9. Examples of the consequent differential horizontal orbit measurements and corrections. The difference between the measured and calculated values at negative and positive action of the corrector was diminished on the basis of the virtual model.

At the entrance to the transport line from the Booster to the Nuclotron, the C^{4+} ions were stripped to C^{6+}.

The photo of the stripping station is presented in Fig. 10. The stripping station was designed and fabricated at BINP. It permits to choose one of three stripping foils remotely without opening vacuum chamber. During this run, three copper foils of a thickness from 10 to 150 μm and aperture of 50×70 mm^2 were installed.

The details on the design of the beam transportation from the Booster to the Nuclotron are presented in Addendum #3.

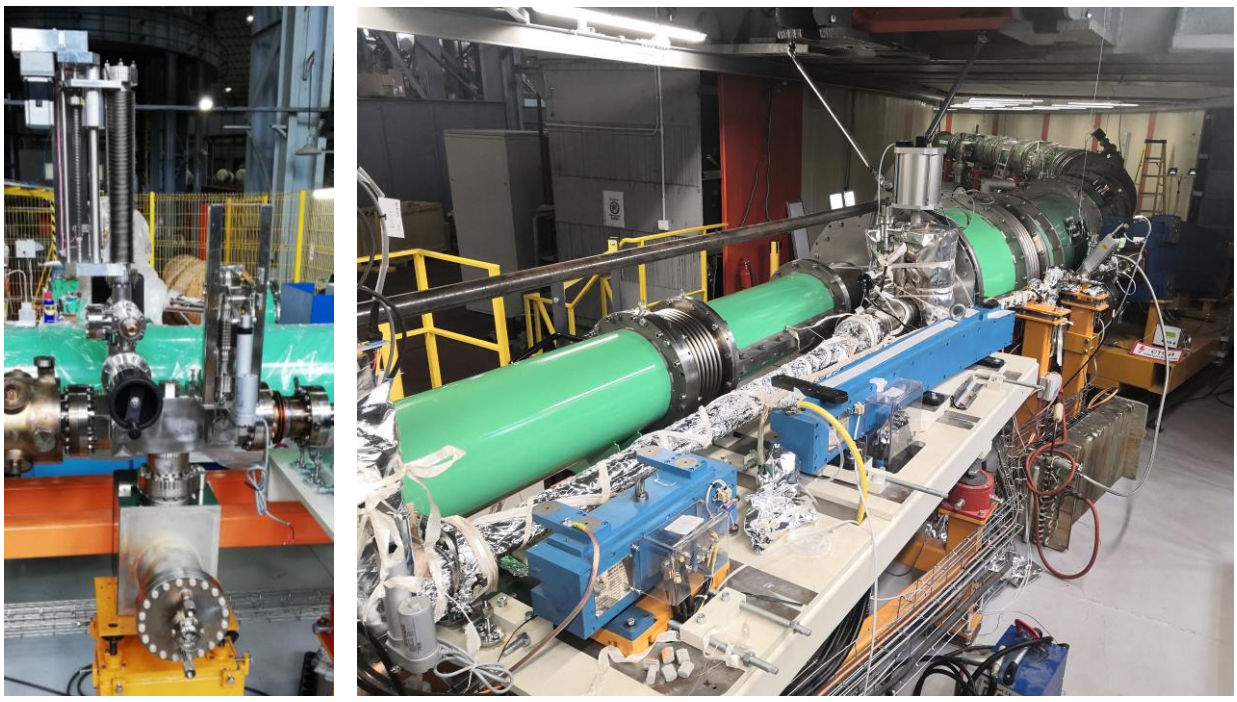

Fig. 10. Stripping station and extraction system.

The commissioning of the new injection kicker and Lambertson magnet was provided during tuning of the beam injection from the Booster into the Nuclotron.

A large amount of the new equipment determined a risk of malfunction or unstable work. To ensure the test of the power supply system of the extracted beam lines and implementation of the experimental program, in addition to the tuning of the injection from the Booster, the LU-20 accelerator together with an additional laser source were prepared for carbon acceleration and injection into the Nuclotron avoiding the Booster. Fortunately, it was not required during this run.

The RF systems of the Booster and Nuclotron were not synchronized in this run, therefore the injected beam initially became scattered when circulating with the Nuclotron RF being switched off, then it was adiabatically captured at the 5^{th} harmonics. In this run, the maximum beam energy of 3 Gev/u was determined by requirements from the planned experiment.

After realization of the slow extraction at spill duration of 6 sec, the new power supply, diagnostic and control systems of the beam transport line to BM@N area were commissioned. Some details about the new beam lines and stations for applied research based on ion beams extracted from the Nuclotron are presented in [4].

As a result, the stable operation of the complex for the SRC experiment was provided during about 24 days.

The total time of the facility operation during the run was about 2150 h.

The achieved transfer efficiency at acceleration from the ion source to the Nuclotron exit was about 25% (Fig. 11). Its main limitations were the pulse-to-pulse variation of the injected beam parameters (explained by the physics of the laser source) and non-optimal stripping target thickness.

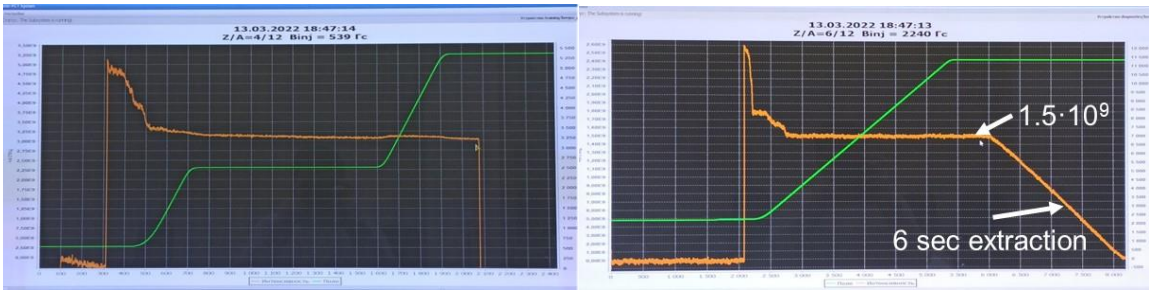

Fig. 11. Parametric current transformer (PCT) signals of the circulating beam in the Booster (left) and Nuclotron (right). The beam intensity at injection into the Booster is $5 \cdot 10^9$ ions.

4. Period between the third and fourth runs

In April, the laser source at HILAC was dismounted, KRION-6T was transported from the test bench to the accelerator building. The main parameters of the KRION-6T are presented in Addendum #1. On April 28, the run at the HILAC accelerator was started for the optimization of Ar and Xe generation and acceleration (Fig. 12).

Fig. 12. KRION-6T mounted on the High Voltage platform

The separators at the liquid helium facility were reassembled to exclude the problem of the previous run.

The Nuclotron cryo-magnetic structure was sufficiently modified in order to prepare the room for the installation of elements of the fast extraction system required for beam injection into the collider. One of the Nuclotron RF stations was removed into another straight section and one of the structural quadrupole magnets was replaced by the new one.

An additional 10 μm thick foil of Ti was installed at the stripping station.

To avoid dilution of the beam during its transportation to the BM@N area, new elements of the vacuum chamber of the channel and the beam diagnostic system including beam profile monitors located in vacuum were manufactured and prepared for test and assembly. The commissioning of the new diagnostics is planned for the 4th technological run as well as the assembly of the vacuum pipe at the entire length of the transport channel.

By June, all the collider dipole magnets were installed and mechanically adjusted in the collider tunnel, connected in pairs to each other (Fig. 13). The assembly of the collider is postponed until the completion of engineering infrastructure mounting that is expected at the end of May 2023.

Fig.13. The collider arc dipole magnets in the tunnel.

The tuning of the collider RF stations was continued at test benches at JINR [5]. The test assembly of the collider electron cooling system was started in October in Novosibirsk (Fig. 14).

Fig. 14. Assembly of the collider electron cooling system at BINP.

One of the goals of the Collider commissioning run (planning for 2023) is to test the power supply system. Each collider ring has its own power supply system based on 3 current

sources PIT11-50, PIT01-40, PIT0.6-30. The main parameters of the sources are given in the Table 1.

Table 1.

Parameters of the Main Current Sources

	PIT 11-50	**PIT 01-40**	**PIT 0.6-30**
Supply voltage Un	3f ~50 Hz 380/220 V		
Peak power, kW	600	45	25
Source voltage, VDC	+/−50	+/−40	+/−30
Maximal current, kA DC	11	1	0.6
Current stability at dI/dt not equal to zero	$2 \cdot 10^{-4}$		
Minimal duration of the rise/fall of the field, s	18		
Current stability at dI/dt=0	$2 \cdot 10^{-5}$		
Maximal duration of the field plateau, hour	24		

2 sets of sources for both collider rings are manufactured by NPP "LM Inverter" and delivered to JINR (Fig. 15).

Fig. 15. PIT 11-50 power supplies

The main elements of the quench protection system are electromechanical switches. The switches are connected in series with structural magnets, 6 switches per each collider ring. All 12 switches are manufactured (Fig. 16).

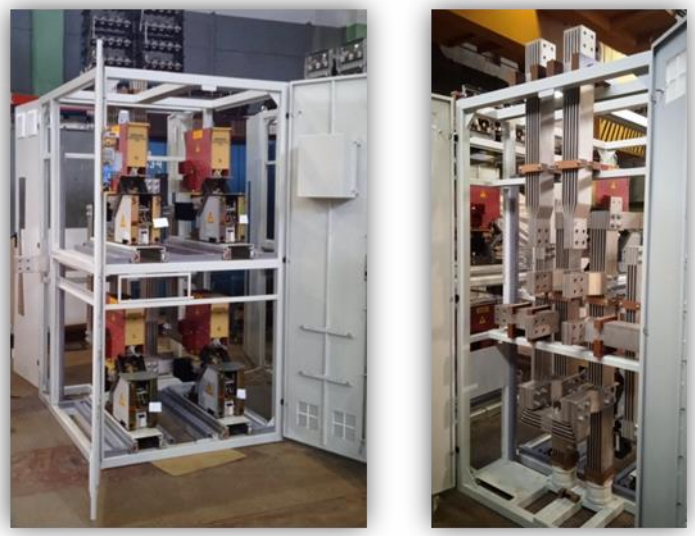

Fig. 16. Energy evacuation switches.

The works to create a power segment from the 6kV/400V network in the process of implementation (Fig. 17).

Fig. 17. 15.11.2022: Installation of the 1.6 MVA transformer in the chamber of building 1A.

5. The fourth run

The 4th commissioning run started on September 20. The cooling of the rings was provided in two steps: the Booster was cooled down to superconductivity temperature, the Nuclotron - down to the temperature of the liquid nitrogen. The cooling of the Nuclotron was completed after the tuning of the Booster. At the initial stage, the Booster operated with argon ions. For the first time at the VBLHEP accelerator complex, the dynamic orbit correction (Fig. 18) was implemented in both – horizontal and vertical planes within the accuracy of about ±5 mm.

In October, a test of the SOCHI station with Ar12+ was performed. The ion beam of a diameter of 100 mm was formed with homogeneity of dose distribution better than 10% on the chip size of 20□20 mm. The microchips XC6SLX16 were irradiated by Ar12+ at an ion energy of 3.2 MeV/n. The cross section of single event effects (SEE) was 1,9□10-2 cm-2 at ion fluence of 3.5□104 ion/cm2.

After that, the Booster was tuned for acceleration of 142Xe28+ ions, the intensity of the accelerated beam was achieved at the level of 2□107 particles. After cooling of the Nuclotron, test of its quench protection system and tuning of the field cycle, the tuning of the beam injection into the Nuclotron started.

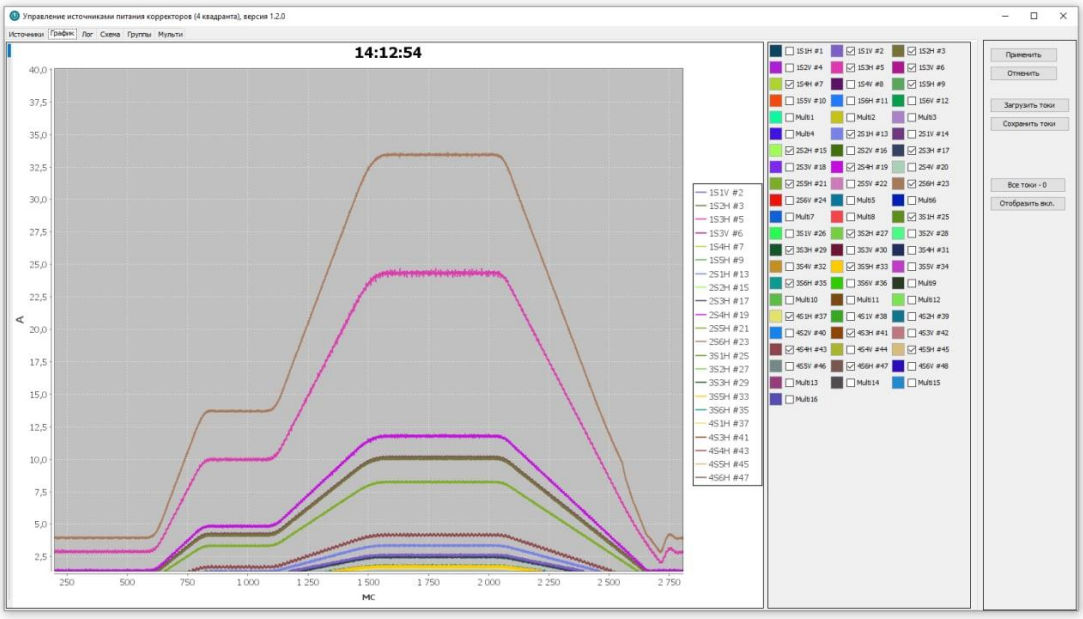

Fig. 18. The panel of the control system for the Booster dipole correctors. Time profile of the corrector currents during the cycle of the Booster.

After the optimum stripping target was chosen, the transport line was tuned for Xe^{54+}. The tuning of the Nuclotron working point and orbit correction at the injection energy permitted to achieve stable beam circulation in the Nuclotron (Fig. 19) at an intensity up to 10^7 particles.

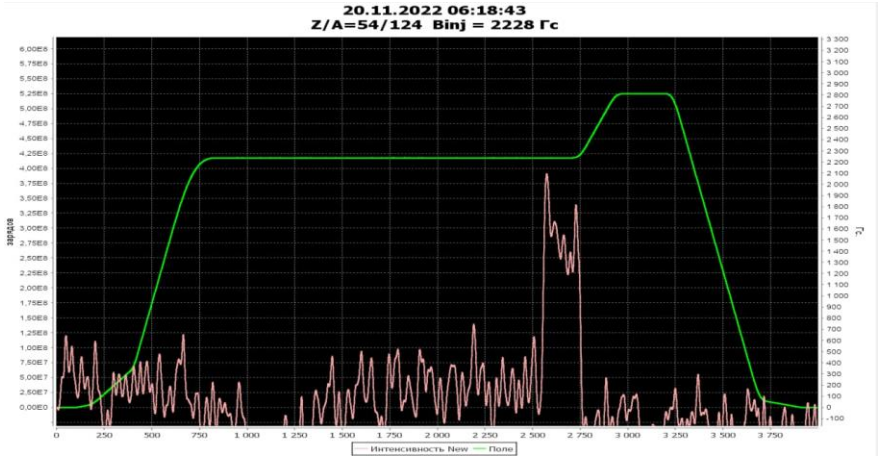

Fig. 19. The Nuclotron PCT signal, the intensity of the circulating Xe beam is about $6 \cdot 10^6$ ions. Tuning of the acceleration is in progress.

In this run, the RF systems of the Nuclotron and Booster were synchronized and for further acceleration the beam from the Booster was injected into the basket at the 4th harmonics of the Nuclotron RF (Fig. 20). The injection was provided at the field plateau. At the beginning of the field growth, the RF amplitude was increased correspondingly to keep the captured particles inside the separatrix.

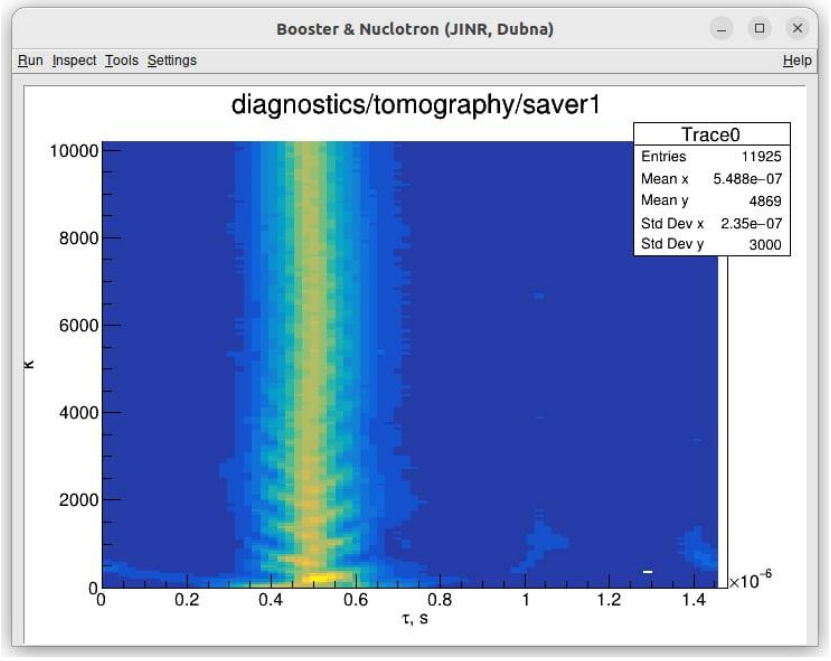

Fig. 20. Beam tomography during its injection into the Nuclotron.

Fig. 21 shows the example of the time dependence of the beam intensity during its acceleration in the Nuclotron.

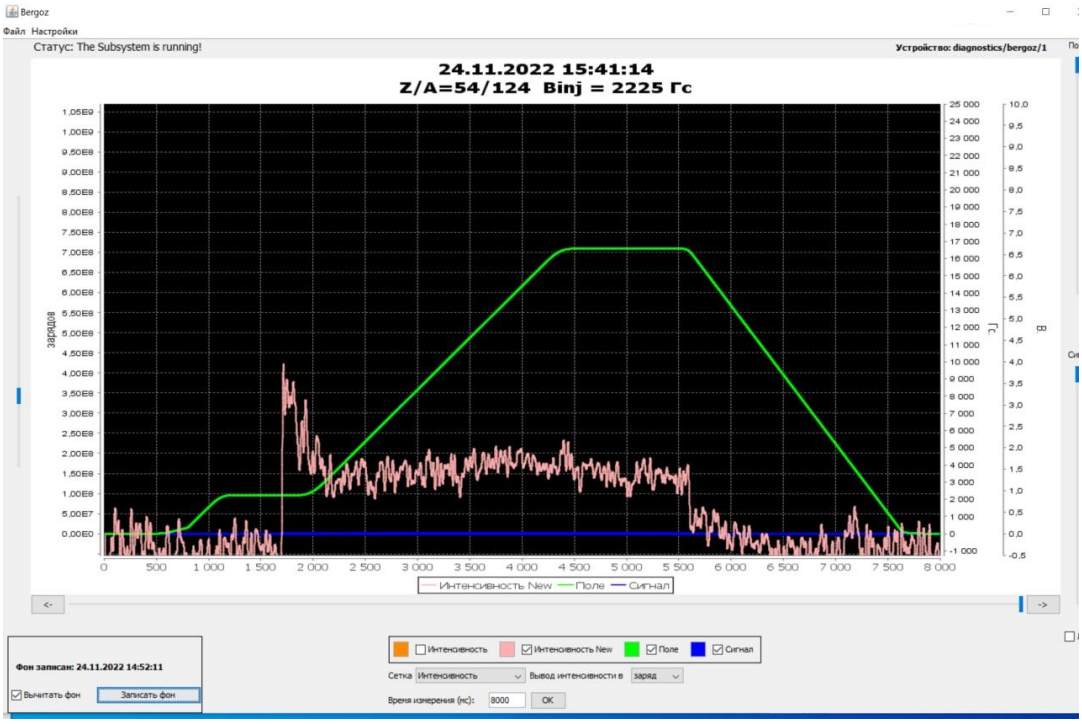

Fig. 21. Beam acceleration in the Nuclotron up to 1.65 T magnetic field plateau (about 3.6GeV/u). Intensity of the accelerated beam is about $4 \cdot 10^6$ ions.

On November 29, the beam was extracted at the energy required for commissioning of the new diagnostics and for realization of the BM@N experiment (Fig. 22). The tuning of the slow extraction is now in progress (fig. 23).

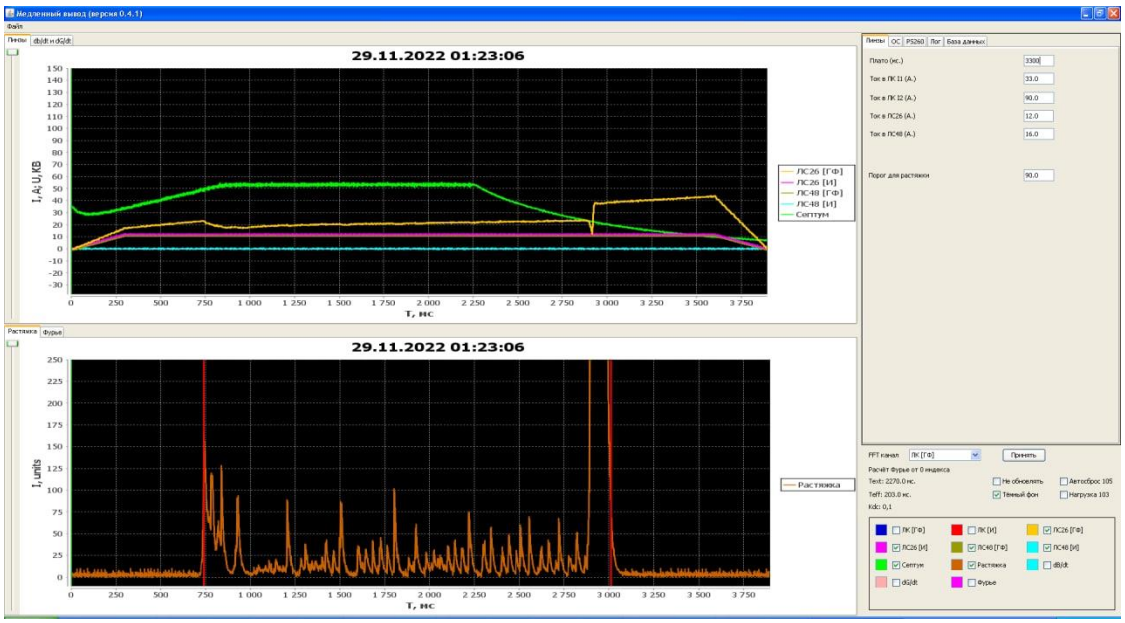

Fig. 22. The first implementation of the Xe beam extraction from the Nuclotron at 3.6 GeV/u. The upper plot - signal of the electrostatic septum Voltage, the currents of the quadrupole and sextupole at the slow extraction. Bottom plot - the extracted beam spill.

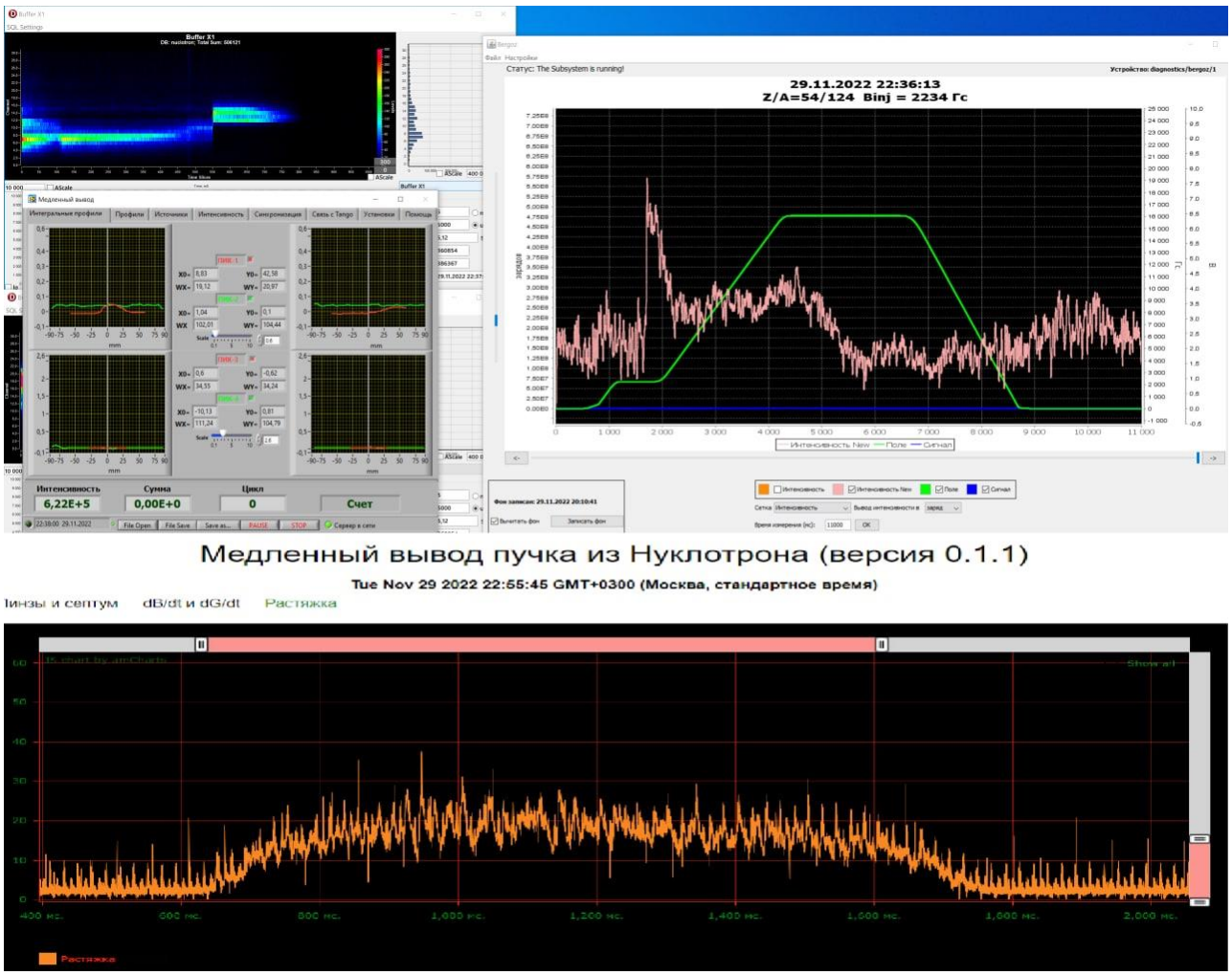

Fig. 23. Diagnostics of the beam acceleration in the Nuclotron and slow extraction into the transport channel of the experimental building. Left upper corner – the horizontal beam position and profile measured with the ionization profile monitor. Below – the beam profiles in the extracted beam line. Upper right corner – the beam intensity (in elementary charges) during the acceleration and extraction measured with the parametric current transformer. The spill of the extracted beam at the exit of the Nuclotron is shown in the bottom plot.

The following actions to be performed by the end of the run:

— tuning of the slow extraction,

— calibration of the new diagnostic system in the extracted beam line,

— reassembling of the vacuum system of the extracted beam line,

— transportation of the beam to the BM@N area and accelerator operation for realization of the experimental program.

List of publications

1. A. Slivin, A. Agapov, A. Baldin, et.al, COMMISSIONING OF THE SOCHI APPLIED STATION BEAM AND BEAM TRANSFER LINE AT THE NICA ACCELERATOR COMPLEX, Proceedings of IPAC2022, Bangkok, Thailand, 2673-5490, 2022
2. D.A. Zolotykh, I.I. Donguzov, S.A. Kostromin, I. Nikolaichuk, T. Parfylo, M.M. Shandov, A.V. Shemchuk, E.V. Zolotykh, V.V. Borisov, O. Golubitsky, H.G. Khodzhibagiyan, B.Yu. Kondratiev, Serial Magnetic Measurements of the NICA Collider Twin-Aperture Dipoles. The Main Results, Proc. RuPAC2021 (Alushta, Russia: 2021).
3. Butenko A V, Brovko O I, Galimov A R, Gorbachev E V, Kostromin S A, Karpinsky V N, Meshkov I N, Monchinskiy V A, Sidorin A O, Syresin E M, Trubnikov G V, Tuzikov A V, Philippov A V, Khodzhibagiyan G G "NICA Booster: superconducting synchrotron of a new generation" *Phys. Usp.*, accepted Issue 11, 2022G.
4. Filatov, A. Slivin, A. Agapov, et.al., BEAM LINES AND STATIONS FOR APPLIED RESEARCH BASED ON ION BEAMS EXTRACTED FROM NUCLOTRON, Proceedings of IPAC2022, Bangkok, Thailand, 2673-5490, 2022
5. Syresin E., Brovko O. I., Butenko A. V., et.al., NICA ION COLLIDER AND PLANS OF ITS FIRST OPERATIONS, Proceedings of IPAC2022, Bangkok, Thailand, 2022.

Addendum #1

Elements of the injection complex, SOCHI station

Injection complex (Fig. 1) consists of two independent parts:

- injector of light ions into the Nuclotron;
- injector of heavy ions into the Booster.

Injector of light ions into the Nuclotron includes:

- light ion source (Helium ion source);
- source of polarized ions (SPI);
- laser ion source (LIS);
- linear accelerator, consisting of Radio Frequency Quadrupole section (RFQ) and Alvarez type drift tube linac LU-20M;
- required beam transport lines.

In the full configuration of the NICA facility the linear accelerator will be replaced by new Light Ion Linear Accelerator (LILAc), which is under construction now.

Injector of heavy ions into the Booster includes:

- heavy ion source “KRION”;
- Heavy Ion Linear Accelerator (HILAc), consisting of Radio Frequency Quadrupole section (RFQ) and two sections of drift tube linac (IH DTL);
- required beam transport lines.
-

In this document the description of the injection elements used in 2021 – 2022 is presented.

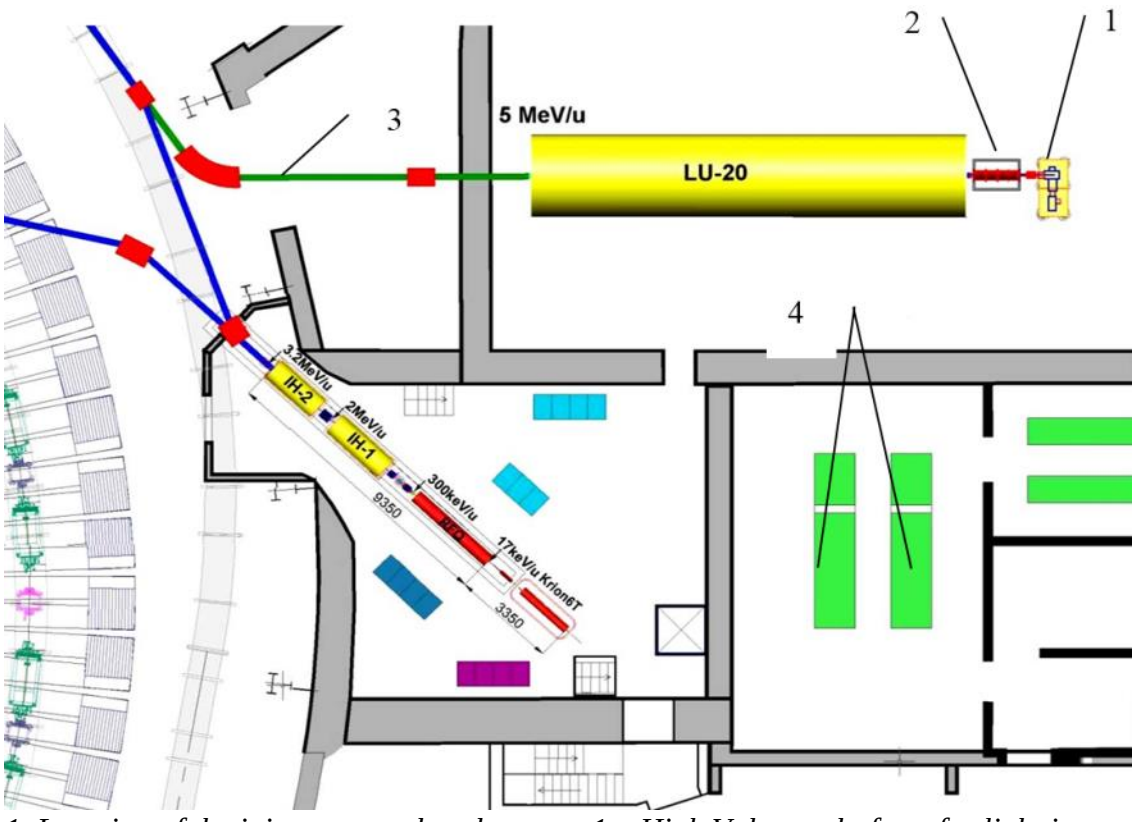

Fig. 1. Location of the injector complex elements: 1 – High Voltage platform for light ion source, LIS and SPI; 2 – RFQ foreinjector; 3 – beam transport line from LU-20M to Nuclotron; 4 – LU-20M RF amplifier.

1. Laser source

The laser source of light ions, developed at the JINR Laboratory of High Energy Physics in 1983, is based on a CO_2 laser. The principle of its operation is based on the extraction of ions from the laser plasma formed as a result of the action of a focused laser pulse on the target. The radiation flux density at the target was ~10^{10} W/cm. and the spectrum of accelerated ions was ${}_6Li^{3+}$, ${}_7Li^{3+}$, B^{4+}, C^{4+}, N^{5+}, O^{6+}, F^{7+}, Mg^{8+}, Si^{11+}.

To obtain ions with a higher charge state, two Nd-YAG lasers were purchased in UK and included into the laser source and test bench for the source parameter optimization. The flux density of laser radiation at the target is estimated to be ~10^{13} W/cm. The tests of the laser at the stand confirmed the presence of six charge states of ions in the carbon plasma. Thus, the new laser source can be configured to produce both light ions of high charge states and ions with a low Z/A ratio for independent operation of both accelerators – the Booster after acceleration in the HILAC (Fig. 2) and the Nuclotron after acceleration in LU-20 or LILAC in the future.

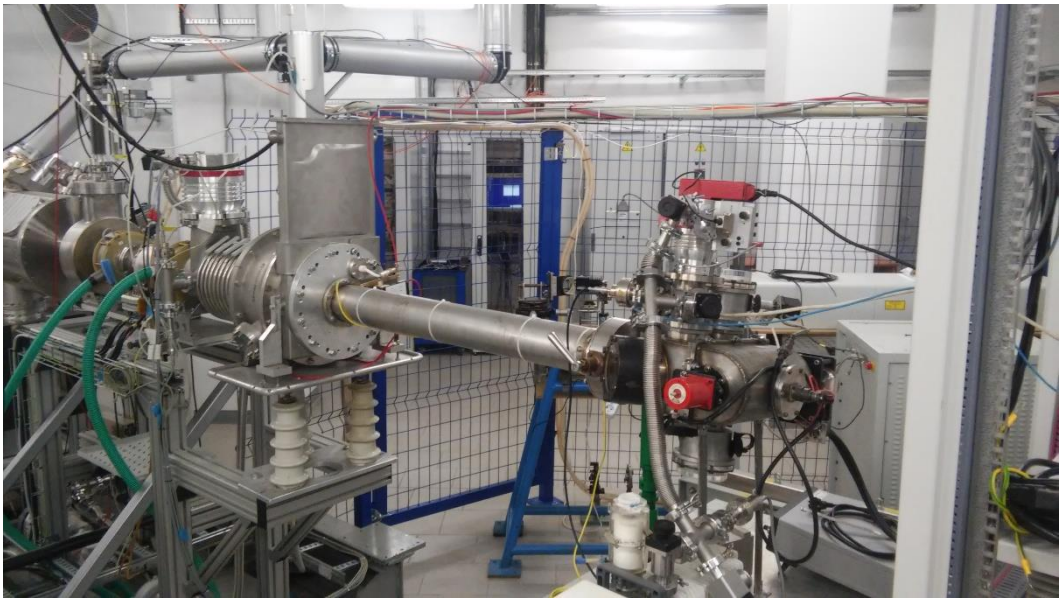

Fig. 2. Laser Ion Source joined with the LEBT in the HILAC's hall

2. Heavy ion source "KRION"

Beams of heavy ions with a high charge states will be produced by the electron-string source (ESIS) "KRION". This source was developed in JINR and based on the phenomenon discovered during the study of operating modes of the electron-beam source EBIS, operating in the reflective mode. It was found that under certain conditions, the "cloud" of repeatedly reflected electrons enclosed in a strong solenoid magnetic field exhibits property similar to the phase transition. This leads to a gradual increase in the electron plasma density and the transition

to a new stationary state called the electron string. While developing the basic version of the NICA facility the “stand” version of the source KRION-6T was constructed. During the operation run of the Nuclotron in 2018, the beams C^{6+}, Ar^{16+} и Kr^{26+} were used, and the operating modes of the source were also investigated (Fig 3.).

Fig. 3. KRION-6T at injector facility during the Nuclotron run in March 2018

The construction of the “KRION – 6N” source for the complete NICA configuration is progressing.

The source “KRION-N” (Fig. 4) is the cryogenic ultra-high vacuum ionizer with 6 T superconducting solenoid. It has three temperature terminals (4.2 °K, 40 °K and 300 °K) and consists of:

- electron-ion-optic system;
- cryo-magnetic system;
- cryogenic vacuum system;
- system for injection of a working substances into the electron string;
- electric power and control systems.

The source length is 1460 mm. Additionally one presumes construction and installation diagnostic devices for measurement of emittance and for analysis of charge state composition of the extracted beam.

Parameters of the NICA ion sources are summarized in Table 1.

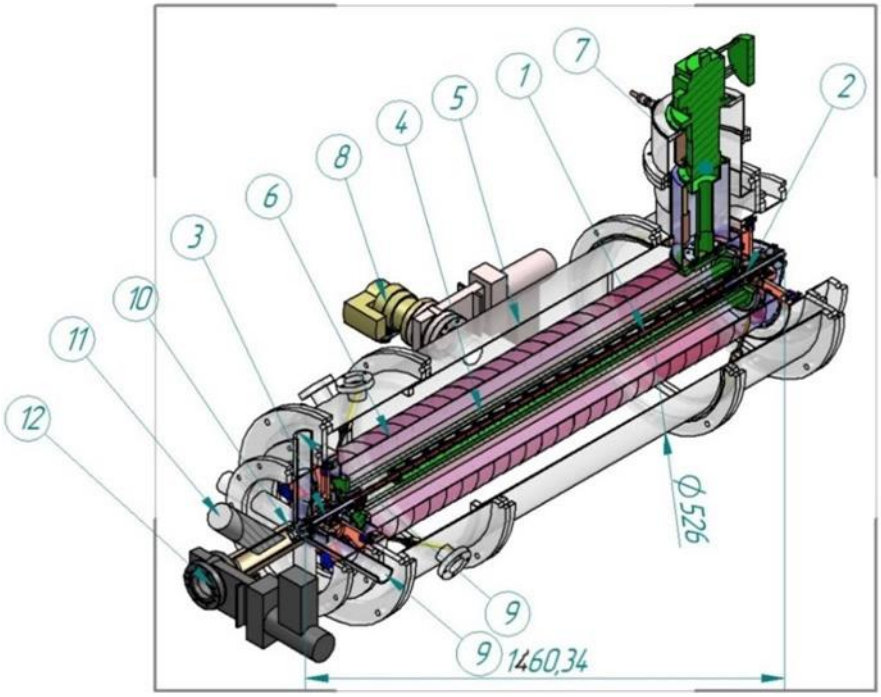

Fig. 4. Ion source "KRION-N": 1 – elements of the electron-ion optic system located along the solenoid axis, 2 – electron gun and 3 – electron reflector, located outside the solenoid in the residual magnetic fields of $B_{max}/20$, 4 – 1200 mm superconducting solenoid, 5 – external vacuum vessel, 6 – copper thermal shield, 7 – head of cryo-cooler, 8 – vacuum valve, 9 – chamber for movable detectors, 10 – electrostatic lens for control of extracted ion beam, 11 – entrance of time-of-flight analyzer, 12 – vacuum valve at the entrance into accelerating section

Table 1.

Parameters of particle sources of NICA injection facility

Source	KRION-6N	Laser source	Duoplasmotron	SPI
Particles	Au^{31+}	Light ions up to Mg^{10+}	H^+, D^+, He^{2+}	$\uparrow H^+$, $\uparrow D^+$
Particles per cycle	$\sim 2.5 \cdot 10^9$	$\sim 10^{11}$	H^+, $D^+ \sim 5 \cdot 10^{12}$ $He^{2+} \sim 10^{11}$	$5 \cdot 10^{11}$
Repetition, Hz	10 (3 pulses for 5 sec)	0.5	1	0.2

3. Heavy ion linear accelerator HILAC

The HILAC (Fig. 5) provides heavy ion (up to U) at the charge to mass ratio ≥ 0.16 for:

- further injection into Booster;
- applied researches area developed for investigation of radiation damages in microelectronics; heavy ions with the energy of 3.2 MeV/u will be used for irradiation of decapsulated microchips.

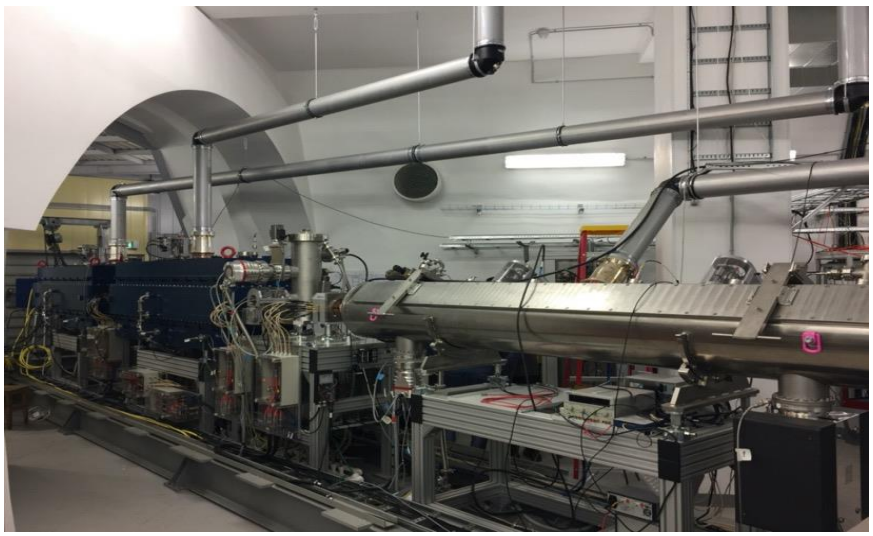

Fig. 5. The HILAc at the accelerator complex

The injector of heavy ions into the Booster based on HILAC includes:

- low energy beam transport line (LEBT), consisting of accelerating tube, two magnetic axial lenses and beam diagnostic box;
- RFQ section, accelerating ions up to 300 keV/u;
- medium energy beam transport line, including two dublets of quadrupole lenses and buncher;
- two IH DTL sections, with quadrupole dublet in between, providing 3.2 MeV/u of the output energy;
- beam transport line from HILAc to Booster, including debuncher.

The HILAC includes the following main systems:

- low level RF system,
- powerful RF system on the basis of solid state amplifiers at 100.6 MHz and total pulsed power of about 1 MW,
- vacuum system,
- power supply system for quadrupole lenses,
- water cooling system.

Arrangement of the beam control and diagnostic system units of the heavy ion injector is presented in Fig. 6.

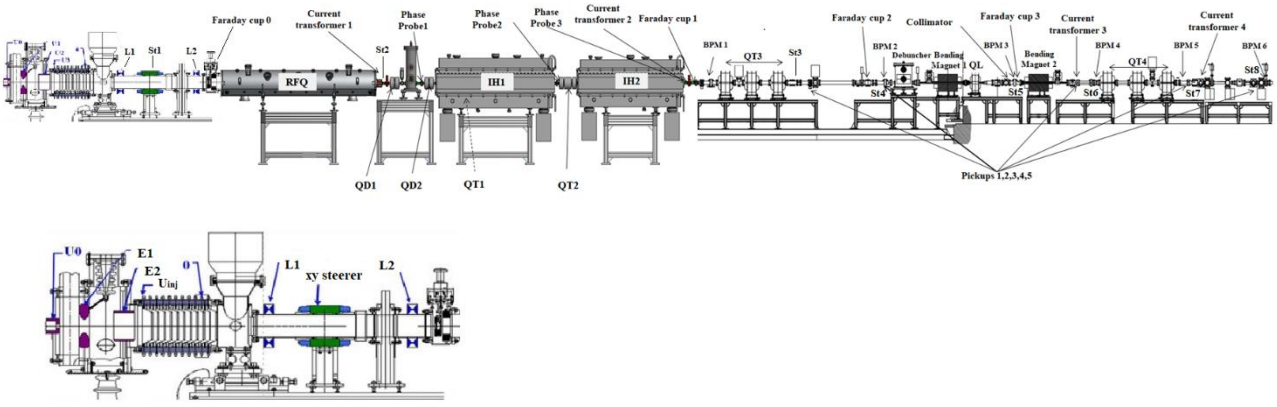

Fig. 6 Layout of the beam control and diagnostic system

In 2015 the HILAC was installed in the workplace in the hall of the injection complex. In 2016 first beam acceleration was demonstrated. In 2018, a series of tests on HILAC commissioning had been carried out to measure the energy spectrum and estimate transmission.

In November 30, 2020, during the first commissioning run the single-component beams of He^+ (mass-to-charge ratio A/Z=4) were accelerated by HILAC up to energy 3.2 MeV/u and injected into the Booster. The intensity $7 \cdot 10^{10}$ of the ions accumulated in the ring per one pulse of injection and accelerated up to 100 MeV/u was achieved.

The second commissioning run in 2021 also started from the He^+ ion acceleration. Transmission 50% was observed for 7 mA beam current at the 8 μs duration at the RFQ output. Beams of He^+ ions were followed by acceleration of Fe^{14+} ions generated with the LIS. HILAC tunings had not been changed when changing ion source because of identical mass-to-charge ratio A/Z=4 both for He^+ and Fe^{14+} ions. Current duration for Fe^{14+} ions ~1-2 μs featured for LIS was observed through injection chain and beam transmission.

4. Beam transport line from HILAC to Booster

Beam transport line from HILAC to Booster includes 7 quadrupole and 2 dipole magnets, debuncher, beam diagnostic devices (Fig. 7), vacuum and power supply systems.

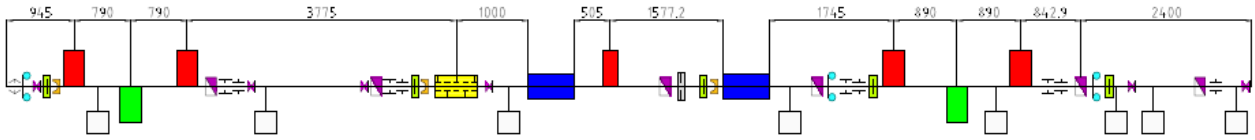

Fig 7. Schematics of the beam transport line from HILAc to Booster

The transport line from HILAc to Booster was mounted during the Booster assembly (Fig. 8). Its commissioning was done successfully during preparation to the first commissioning run of the Booster.

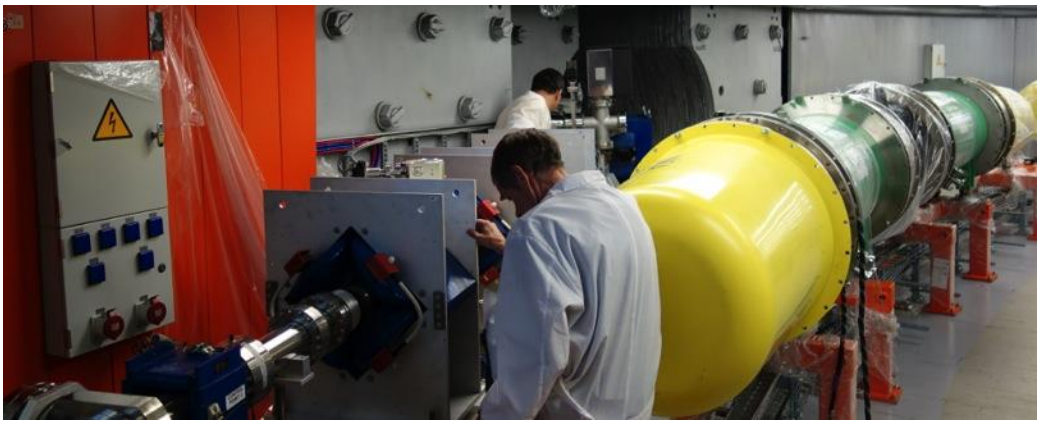

Fig. 8. Elements of the transport line from HILAc to Booster during the assembly

5. Beam transport line from HILAC to SOCHI station. Chip irradiation by low energy ions in SOCHI

Within the framework of the NICA project, the SOCHI station (Station of Chip Irradiation) was constructed for chip irradiation by short-range ions extracted from the HILAC at the energy of 3.2 MeV/n. Additional part of the HILAC-Booster beamline (Fig. 9) is used for beam transportation to SOCHI. A dipole magnet installed in the middle of this channel deflects the ion beams to SOCHI.

Fig. 9. Beamline from HILAC to Booster

The ion energy after the HILAC is insufficient to pass through the microchip-surrounded capsule. Therefore, the chip decapsulation will be done before its irradiation. The $^{197}Au^{79+}$ ions provide the linear energy transfer of 95 MeV·cm^2/mg in the silicon chip at the energy of 3.2 MeV/n. The maximum ionization dose rate during one HILAC beam pulse should be less than 10^6 rad/s in the silicon chip. This requires the reduction of the beam current from milliamperes after the HILAC to several tenth of nanoamperes at the chip location. A diaphragm with several holes of 20 μm in diameter was installed in front of the triplet of quadrupoles in the HILAC-Booster channel (Fig. 10) to reduce the beam current by five orders of magnitude. The HILAC-SOCHI transfer line optics involves a triplet of quadrupole lenses, a dipole magnet, and two

quadrupole lenses. It permits formation of the round-shaped ion beam with the FWHM size of 70 mm on the irradiation target. The beam inhomogeneity is less than 10% at the chip target size of 20×20 mm.

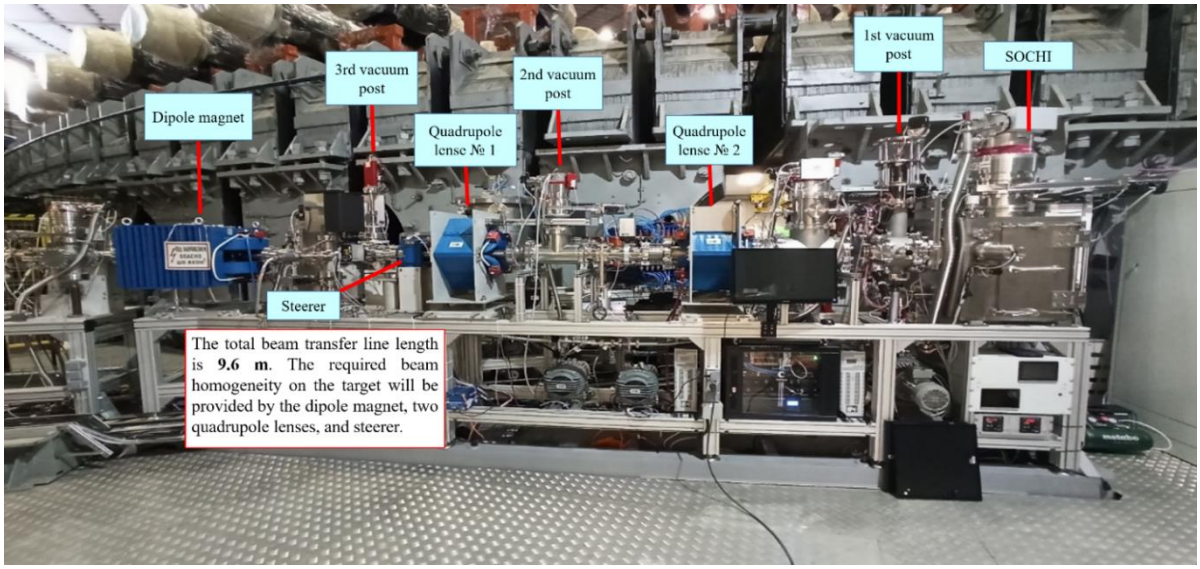

Fig. 10. Beamline HILAc- SOCHI and station SOCHI.

The vacuum pressure in the SOCHI (Fig. 11) will be less than 10^{-5} Torr and 3 orders of magnitude higher than the pressure of 10^{-8} Torr in the HILAC-Booster channel. The HILAC-SOCHI channel was designed to allow differential pumping in the area behind the dipole-deflecting magnet and to prevent heavy gases like CO and H_2O from leaving SOCHI and penetrating into the HILAC-Booster channel. To solve these problems, a cryogenic trap, a pulsed diaphragm crossing vacuum chamber and pumps were installed in this applied channel behind the deflection dipole magnet.

Fig. 11. Station SOCHI.

The diagnostics system is represented by the following detectors: the MCP-based detector and the system for online diagnostics and control of peripheral ion flux density and fluence (four fiber-scintillation detectors based on multi-channel photomultiplier) (Fig. 12); the fast total-absorption scintillation detector with optical readout, the Faraday cup (Fig. 12), and the fast total absorption phosphor detector. The signals from the detectors are integrated into the general data acquisition system.

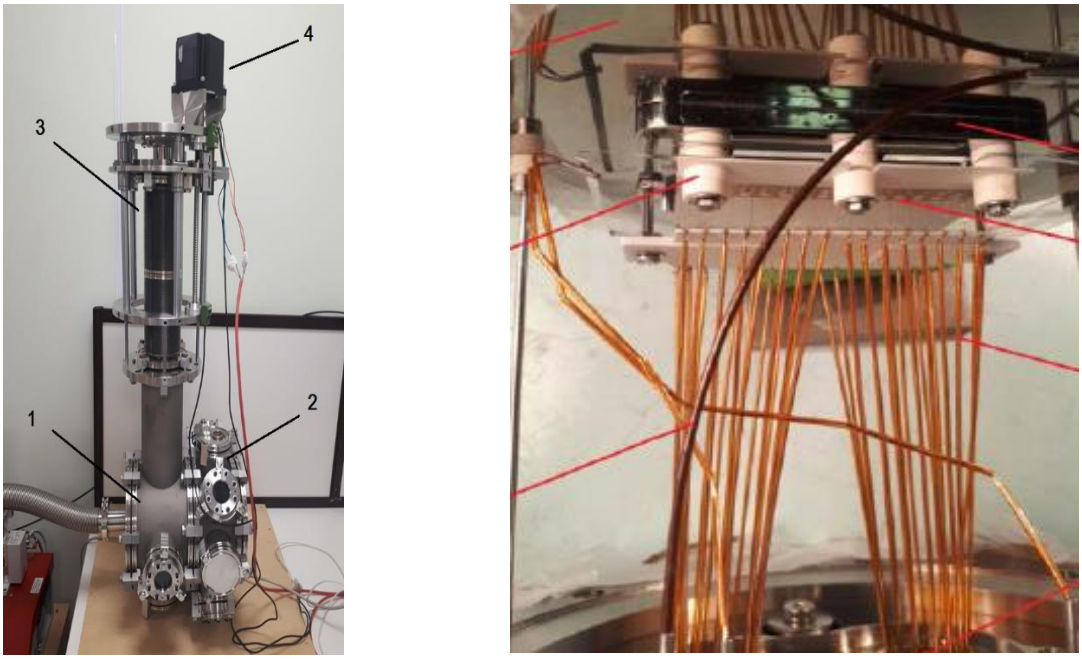

a) *b)*

Fig. 12. a) SOCHI detector vacuum chamber for installation of scintillation detectors, Micro-channel plate detector (MCP) and Faraday cap. b) SOCHI MCP detector.

Table 2 represents main parameters of the SOCHI silicon detector.

Table 2.

Parameters of SOCHI silicon detector

Parameter	Value
Input port diameter, mm	15
Working field, mm	10×10
Ion energy range, MeV/n	3.2
Time variation of ion energy at beam pulse to pulse	±5%
Beam pulse duration, μs	30
Repetition frequency, Hz	1
Area of detector displacement, mm	100 ×100
Accuracy of detector position, mm	1
The beam time structure measurement, polling rate, Hz	20
Fluence measurement	Yes
Space resolution, mm	2-3
Accuracy of beam inhomogeneity measurements	±10%

Addendum #2

Booster synchrotron, results of first runs

Superconducting booster synchrotron (Booster) is the heavy ion injector of the Nuclotron. Main goals of the Booster operation are the following:

- beam storage at injection energy ($2 \cdot 10^9$ ions of $^{197}Au^{31+}$);
- acceleration at minimum loss by achievement of ultra-high vacuum conditions in the beam pipe,
- formation of the required beam phase volume by electron cooling application;
- acceleration of heavy ions to the energy required for effective stripping;
- fast extraction of the beam for injection into the Nuclotron.

The Booster with a perimeter of 211 m and a structure of four periods is placed inside the yoke of the Synchrophasotron magnet (Fig. 1, 2). The maximum field of the Booster dipole magnets is 1.8 T (magnetic rigidity is 25 T·m), which corresponds to the $^{197}Au^{31+}$ions energy of 578 MeV/u.

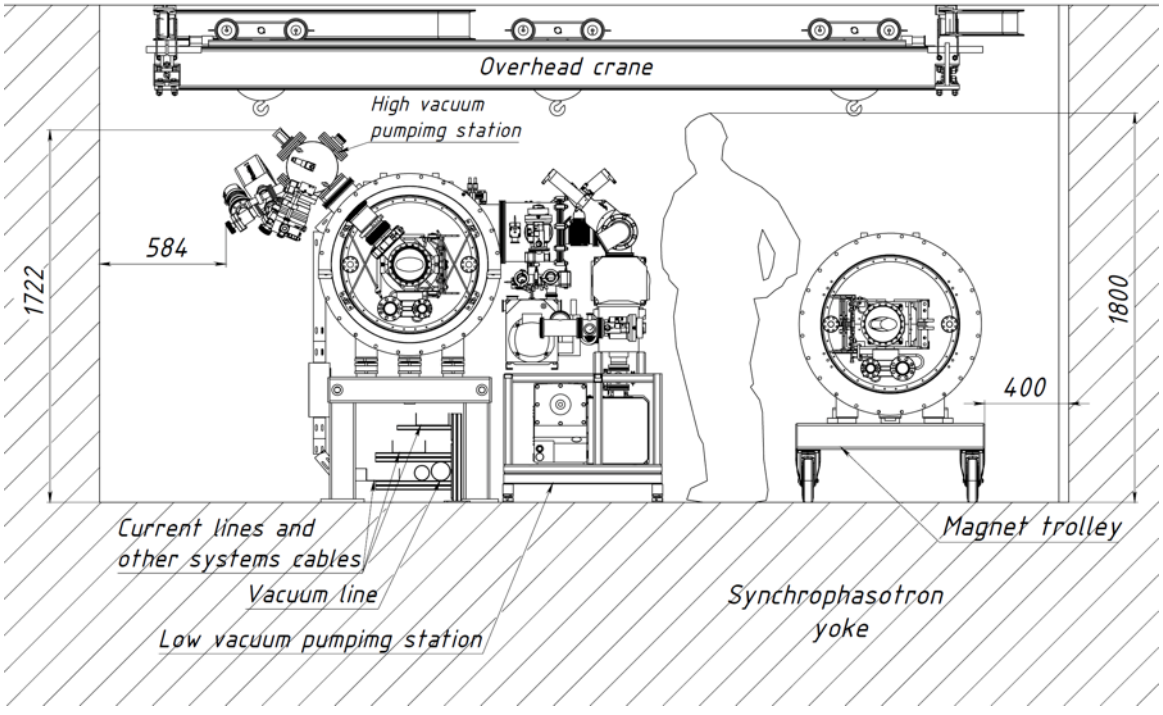

Fig. 1. Location of the Booster magnets inside the yoke of the Synchrophasotron magnet.

Fig. 2. The Booster magnets in the tunnel.

The Booster systems are listed below and shown in Fig. 3.

Cryo-magnetic system, including dipole magnets, quadrupole lenses, correctors, vacuum chambers, cryostat system. The magnetic structure of the Booster consists of 4 superperiods, each includes 5 regular periods and one period that does not contain dipole magnets. The regular period includes focusing and defocusing quadrupole lenses, 2 dipole magnets, and 4 small free straight sections designed to locate multipole correctors, collimators, and diagnostic equipment. The listed elements of the magnetic system belong to the structural elements of the Booster. Periods that do not contain dipole magnets are designed to locate inserted elements. The inserted elements are: the beam injection and extraction systems, the accelerating RF system and the electron cooling system.

The electron cooling system (ECS) of the Booster, designed to form the required value of the phase volume of the beam, has maximum electron energy of 60 keV. The electron cooling system is designed and manufactured in the Budker Institute of Nuclear Physics (BINP, Novosibirsk). ECS includes the following systems: main magnetic structure of ECS, electron gun and collector, magnetic optics, vacuum system and diagnostics of ECS, automated control system of ECS, power supply systems and engineering systems.

Injection and extraction systems, including test benches for their elements.

Power supply system of Booster magnets, including the main and two additional power supplies, power supplies for correctors, energy evacuation system, quench detection system.

Radio-frequency system (RF), including accelerating stations and control system. The Booster acceleration stations were designed and manufactured at Budker INP (Novosibirsk), delivered to JINR and tested at the testbench with a magnetic field cycle imitator in 2014.

Diagnostic and control system including the following subsystems and devices: magnetic field ramp dB/dt measurement system, cycle control system, pickups, diagnostics, orbit correction system, thermometry system, Booster ACS, orbit measurement system, ionization monitor. Additionally, the system includes test benches for the diagnostic and ACS elements.

Vacuum system, including a pumping system of the beam pipe, the pumping system of the insulation vacuum volume and control system of the vacuum equipment. The system also includes high-vacuum stands.

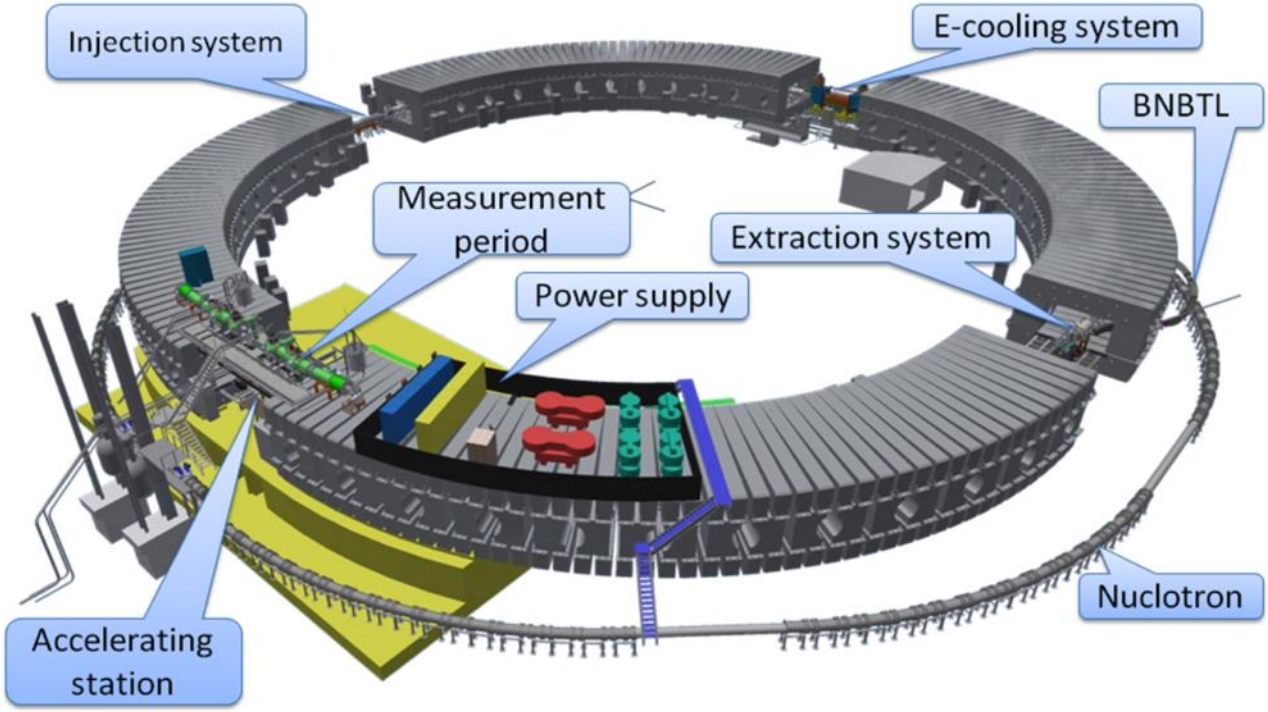

Fig. 3. Location of the main Booster systems

The main parameters of the Booster are listed in Table 1.

Table 1.

Main parameters of the Booster

1. Common parameters	
Ions	$^{197}Au^{31+}$
Injection energy	3.2 MeV/u
Maximum energy	600 MeV/u
Magnetic rigidity at injection	1.6 T·m
Maximum magnetic rigidity	25 T·m
Circumference	210.96 m
Transition energy	3.25 GeV/u

2. Optic structure and magnetic elements	
Number of super-periods	4
Number of DFO periods	24
Number of dipole magnets	40
Number of quadrupole lenses	48
Effective length: Dipole magnets Quadrupole lenses	 2.2 m 0.47 m
Magnetic field of the bending magnets: At injection Maximum	 0.11 T 1.8 T
Gradient of the F lenses: at injection,	1.28 T/m
maximum	21.01 T/m
Gradient of the D lenses: at injection,	–1.31 T/m
maximum	–21.48 T/m
Bending radius in the dipole magnets	14.09 m
Number of long straight sections	4
Length of the long straight section	7 m
Lengths of the small straight sections	0.7/0.85/0.95 m
3. Lattice and beam parameters	
Betatron tunes: Q_x Q_z	 4.8 4.85
Chromaticity: $\Delta Q_x/(\Delta p/p)$ $\Delta Q_z/(\Delta p/p)$	 −5.1 −5.5
Orbit compaction factor	0.05
Amplitude of corrected orbit	4 mm
Acceptance: Horizontal Vertical	 150 π·mm·mrad 57 π· mm·mrad
Beam emittance at injection $\varepsilon_{x,z}$	15 π· mm·mrad
Horizontal emittance after acceleration ε_x	< 11 π· mm·mrad
Vertical emittance after acceleration ε_z	< 1.5 π· mm·mrad
Relative momentum spread at injection	$\pm 10^{-3}$
Maximum momentum spread	$\pm 2.3 \cdot 10^{-3}$
Momentum spread after acceleration	$\pm 2.2 \cdot 10^{-4}$
Revolution period at injection	8.5 μs
After acceleration	0.89 μs

Assembly of the Booster has been started in 2016 with the installation of the electron cooling system in its nominal position. Work on ECS tuning to design parameters is currently in the final stage. The first elements of the booster magnetic system were delivered to the accelerator hall in September 2018.

The Booster assembly was completed at the end of 2019. All elements of the Booster were tested and tuned. The technological run dedicated to the Booster commissioning has been

started on 12 November 2020. The second technological run dedicated to commissioning of fast extraction system, beam transport line from the Booster to the Nuclotron and the electron cooling system of the Booster was conducted in September 2021.

During the first run, completed on 30 December 2020, the following works were performed consequently:

- assembly and test of the vacuum system was completed,
- the Booster control and thermometry systems were put into operation, cryo-magnetic system was cooled down to 4.5 K,
- the quench detection system was tuned and put into operation, cycle control system and power supply system of Booster magnets were tuned,
- the heavy ion linear accelerator HILAC and the beam transport line from the HILAC to the Booster were tuned, the design parameters of the injection system devices were provided,
- the beam injection into the magnetic field plateau corresponding to the injection energy was performed, circulation beam of He^{1+} ions was obtained,
- main systems of the circulating beam diagnostics, orbit correction system were tested consequently, the circulating beam intensity closed to the design value was obtained,
- Radio-Frequency system was tuned, the regime of the adiabatic beam capture into the acceleration was tested, the beam acceleration up to 100 MeV/u was obtained,
- the electron cooling system was switched on and tested,
- the power supply, cryogenic and cryo-magnetic systems were tested at operation with the magnetic field cycle of the design parameters.

The main results of the second run of the Booster beam commissioning (September 2021) are the following:

- the beam injection efficiency with adiabatic capturing at 5th harmonic at efficiency was higher than 95%; the beam was accelerated up to 65 MeV/u and was recaptured with 1st RF harmonic with efficiency closed to 100%;
- acceleration up to the nominal energy of 578 MeV/u with dB/dt = 1.2 T/s;
- ultra-high vacuum in beam pipe ($^4He^{+1}$ ion life-time was more than 10 s),
- electron cooling of Fe ions at energy of 3.2 MeV/n was achieved,
- beam extraction to transport line Booster-Nuclotron and transportation with total transfer efficiency of 70%.

Addendum #3

Beam transport from the Booster into the Nuclotron

The beam extraction from the Buster is provided by the following way. After acceleration to the required energy the bunch length is optimized by appropriate choice of the Booster RF Voltage, the orbit of the circulating bunch is displaced locally close to extraction septum (closed orbit bump), the extraction kicker synchronized with the RF phase displaces the bunch into the septum chamber. The striping target station located at the entrance of beam transport line permits to remotely remove completely the target or use one of three targets of different thickness and material optimized for stripping of different ion species. At the exit of the beam transport line the bunch reaches the beam injection system from the Booster to the Nuclotron.

Beam extraction system is aimed to stripping of ions accelerated in the Booster and the beam transfer into beam transport line to the Nuclotron. Its main elements (kicker and two sections of the septum) are located in the third Booster straight section (Fig. 1).

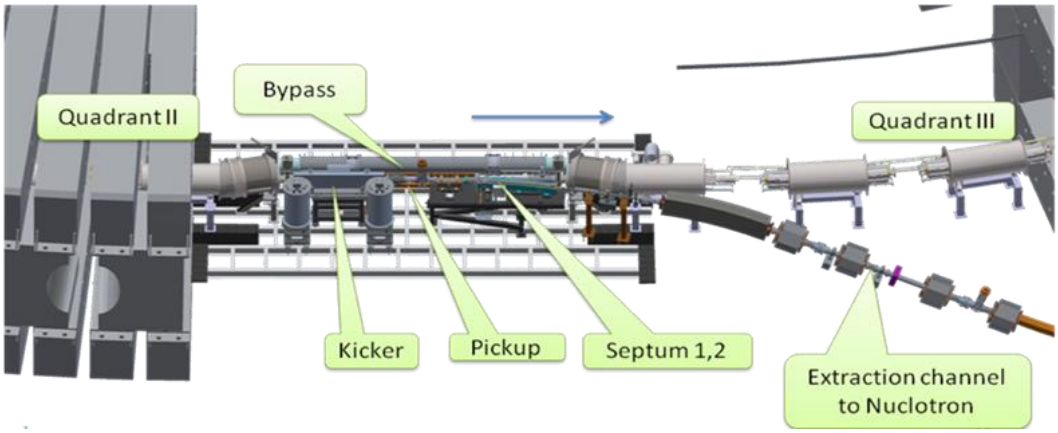

Fig. 1. Location of elements of the beam extraction system.

The extraction system was manufactured in BINP (Novosibirsk). Assembly and test of the extraction system was completed in July 2020 (Fig. 2.).

Fig. 2. Installation of the septum magnet of the fast extraction system

Prototype of the power supply unit for the closed orbit bump used for the fast extraction was completed in October 2020 (Fig. 3). Its assembling at the Booster was completed in July 2021. During the second commissioning run it was put in operation.

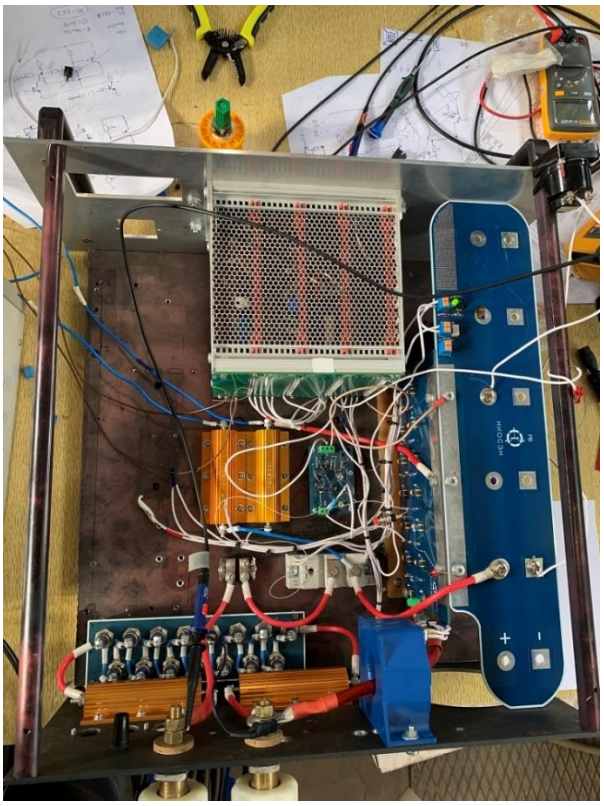

Fig. 3. Prototype of the power supply unit for the closed orbit bump

The Booster-Nuclotron beam transport line (Fig. 4) passes through the magnet yoke of the former Synchrophasotron accelerator, then the channel route descends down to the Nuclotron ring through an opening in the concrete floor above the Nuclotron tunnel. The beam line has a complex three-dimensional geometry, and beam transportation in it is performed horizontally and vertically at the same time. The transport line consists of the main path of ion transfer to the Nuclotron and a branch for the dump of ions of non-target charge state. The optical system of the line consists of 5 dipole magnets, 8 quadrupole lenses, a septum magnet for the dump of ions of non-target charge state and 3 two-coordinate dipole correctors. The total length of the line is 25.5 m. the azimuthal size of the channel is approximately 45°, which corresponds to the injection of a beam through one superperiod (octant) of the Nuclotron from the extraction point of the Booster.

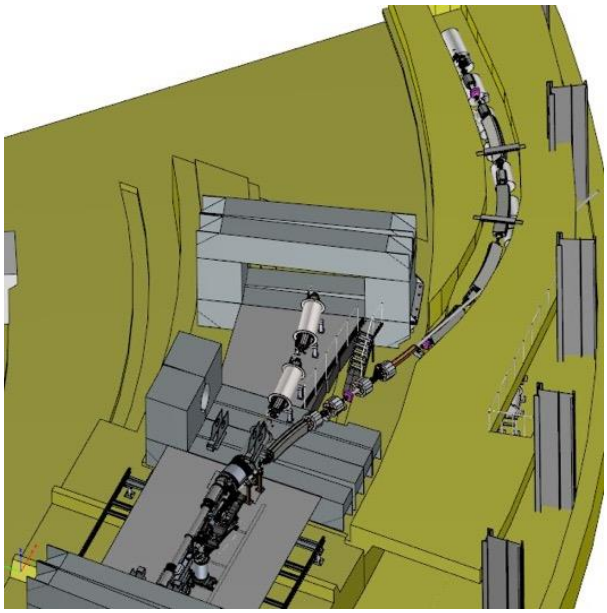

Fig. 4. Artistic view of the region containing the fast beam extraction from the Booster and Booster-Nuclotron transport line

The vacuum system of the Booster-Nuclotron transport line ensures the achievement of an operating vacuum of the order of 10^{-9} Torr along the ion beam pipe of the line, except for the initial section of the line with differential pumping, in which the residual gas pressure reached the vacuum level of the Booster ring of 10^{-11} Torr.

The line was manufactured at BINP and delivered to JINR in June 2021. Its assembly was completed in September (Fig. 5) and commissioning was performed during the second commissioning run.

Fig. 5. Assembly BNTL after the first run. From left to right: installation of magnetic elements, assembly of the kicker power supply, installation of the magnet power supply units.

Optical structure of the Booster around the extraction point is shown in Fig. 6. Four pairs of the Booster dipole magnets are used for excitation of the local orbit distortion during the beam extraction. The stripping station is located in the Booster at the entrance of the first section of the septum magnet.

Optical structure of the line is presented in Fig. 7. The septum magnet SM3 is aimed for separation of the ions at parasitic charge states. The diagnostic system includes 6 beam position monitors (BPM), two fast current transformers (FCT) at the entrance and at the exit of the line, and 3 movable luminescence profile monitors. Additionally, one of the Booster BPMs is used for tuning of the beam transfer and 2 specialized BPMs were installed at the Nuclotron. The beam orbit correction is provided by two-dimension steering magnets.

Location of the beam injection system in the Nuclotron and nearest Nuclotron optic elements are shown in Fig. 8.

Commissioning of the transport line with Fe^{14+} ions was performed during second commissioning run. Signal from BPMs in the transport line are presented in Fig. 9, the beam spot at the luminescence profile monitor – in Fig. 10.

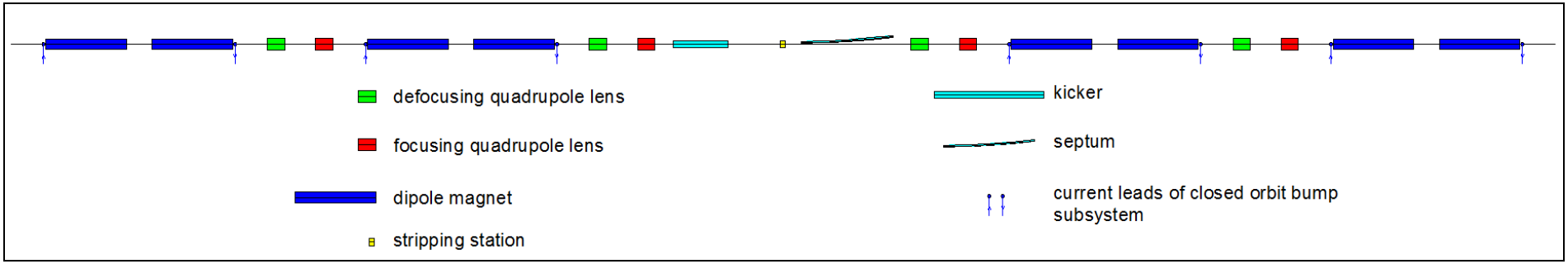

Fig. 6. Optical structure of the Booster around the beam line.

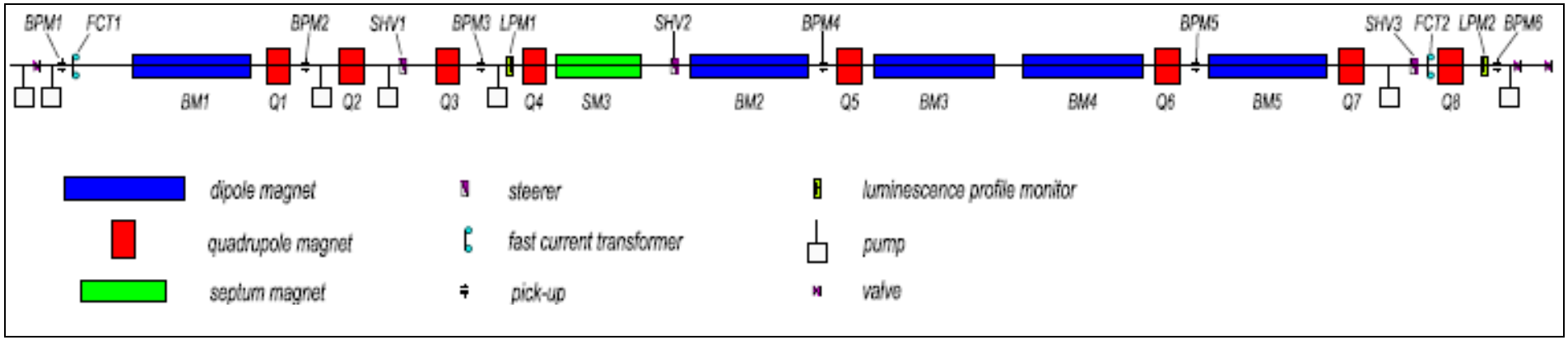

Fig. 7. Optical structure, beam diagnostics and correction system of the Booster-Nuclotron beam line.

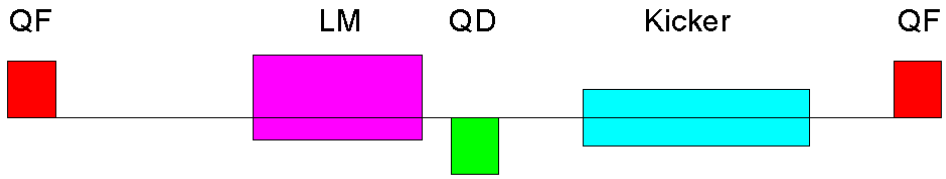

Fig. 8. Location of the beam injection system elements in the Nuclotron straight section.

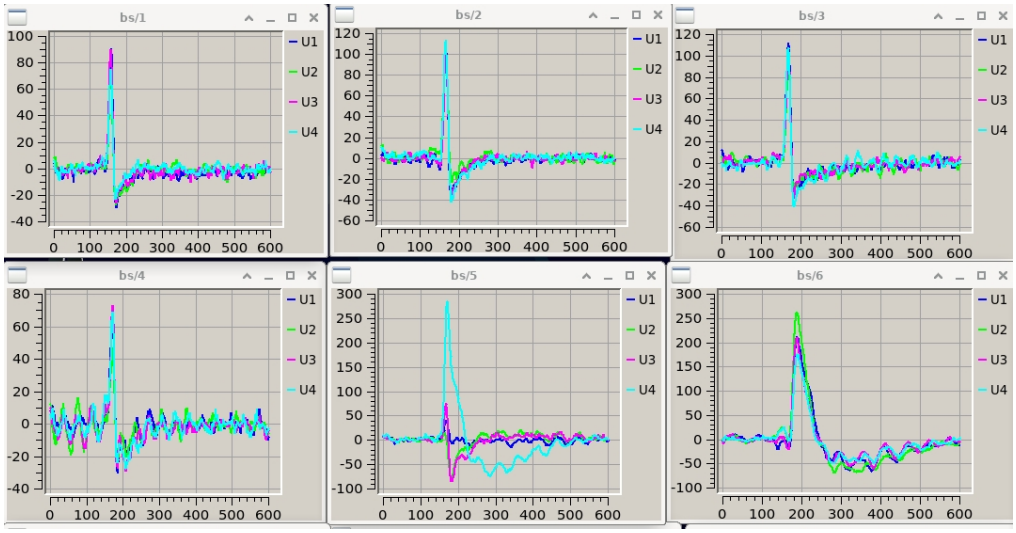

Fig. 9. Signals from BPMs of the transport line at the time of Fe^{14+} ions transportation during second commissioning run.

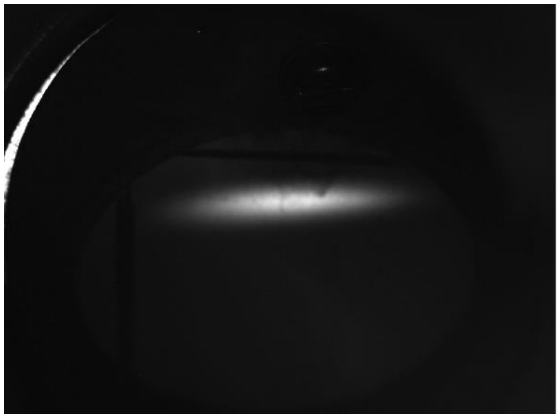

Fig. 10. The beam spot of Fe^{14+} ions at the exit of the Booster-Nuclotron transport line during second commissioning run.

The photo of the stripping station is presented in Fig. 11. The stripping station designed and fabricated at BINP permits to choose one of three stripping foils remotely without opening vacuum chamber. The station was commissioned during third commissioning run, when three copper foils at thickness from 10 to 150 μm and aperture 50×70 mm^2 were installed.

Fig. 11. Stripping station (left) and the stripping foil inside the vacuum chamber (right).

Beam injection system from the Booster to the Nuclotron

The single-turn beam injection system allows to place a bunch transported from the Booster into equilibrium orbit of the Nuclotron. The system consists of a Lambertson magnet and a pulsed ironless dipole magnet – the kicker (Fig. 8).

The Lambertson magnet (Fig. 12) is a dipole magnet with two apertures: the separated areas for the injected and circulating beams. In the first area, a horizontal magnetic field of up to 1.1 T is initiated by superconducting windings that deflects vertically the injected beam. Both areas are separated by steel wall of special form to minimize the scattered magnetic field in the circulation region. To decrease the level of this scattered field even more, a superconducting coil compensating this field is placed. The Lambertson magnet and the compensating coil are operated from individual power supplies.

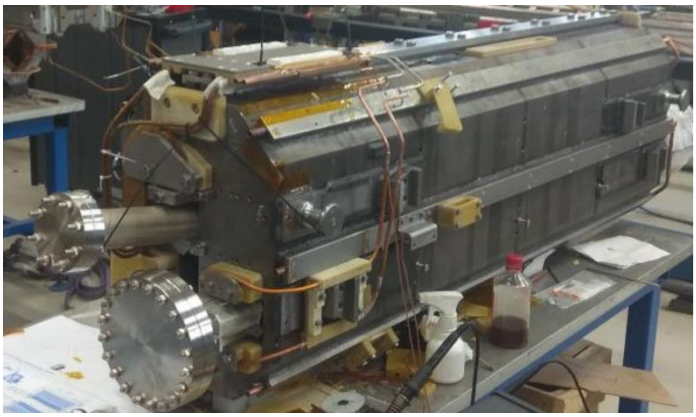

Fig. 12. Assembling of Lambertson magnets at VBLHEP line for assembly and test of superconductiong magnets.

The walls of the vacuum chamber slightly reduce the acceptance of the Nuclotron. To restore it to the initial value during beam injection, the exit of the Lambertson magnet can be shifted by 15 mm.

The kicker of 2 m length (Fig. 13) consists of two pairs of conductors installed inside the vacuum box. The conductors are switched so that they form a magnetic field perpendicular to the plane of the beam orbit. The kicker power supply is pulsed, based on the pulse-forming line. Its repetition frequency is 0.25 Hz, the maximum amplitude of the current pulse is 25 kA. The durations of the leading and trailing edges are less than 500 ns. The duration of the pulse plateau is 500÷700 ns. The injection kicker pulse is synchronized with the Booster extraction one with account to the bunch time of flight through the transport line.

Fig. 13. Nuclotron injection kicker

The main elements of the injection system were designed at VBLHEP. Assembling and commissioning of the injection system elements were performed in November 2021. The beam test was done during the third commissioning run.

Addendum #4

Beam transfer channel to the experimental set-ups in the building 205 and Measurement Pavilion

The beam transfer channel (BTC) is used for beam transportation from the Nuclotron to the BM@N experiment and the Short-Range Correlation (SRC) set-up in building 205 and areas for applied research in Measurement Pavilion (Fig. 1). The length of the BTC from the Nuclotron exit to BM@N is about 170 m. In the past, the pressure in the evacuated part of the channel was 0.1 Pa, and it was higher at 40 m at the location of the air gaps. Such conditions did not meet the experimentalist's requirements for extracted beams (Table 1), they were improved along the length of 110 m. The vacuum chamber diameter is 196 mm. The channel beam diagnostic was modernized and developed as well. New sections of the vacuum chamber of the channel and the beam diagnostic system are manufactured at Belgorod State University.

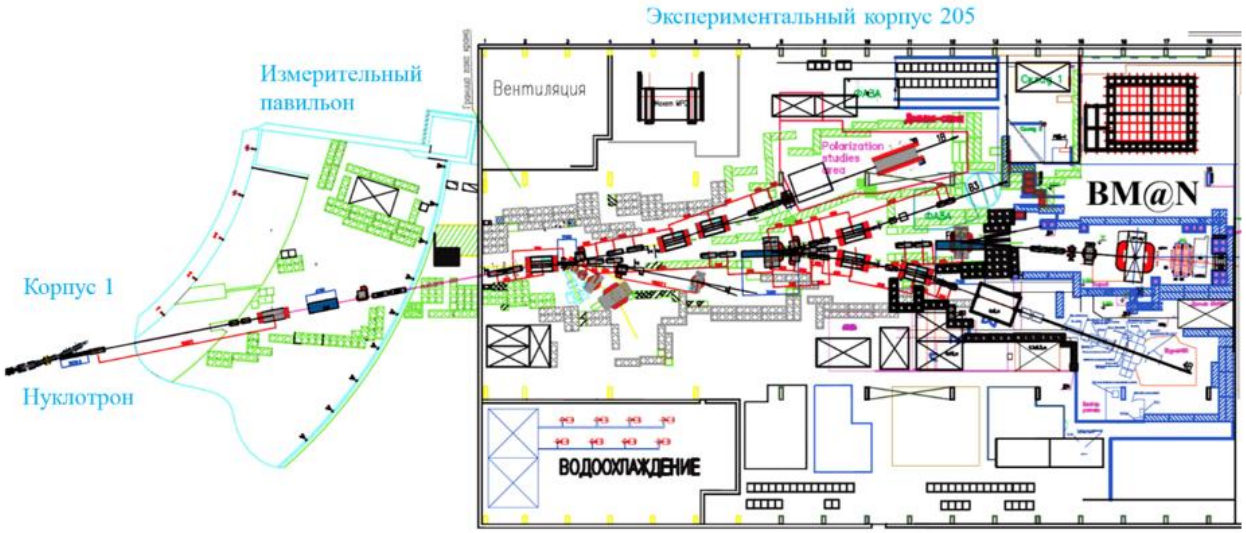

Fig. 1. Scheme of location of the BTL and experimental set-ups in building 205

Table 1

General parameters of the Nuclotron extracted beams

Parameter	Value
Ions	C^{6+}, Kr^{36+}, Au^{79+}
Beam intensity, ion/cycle	$10^4 \div 10^8$
Ion energy, GeV/u	1 ÷ 4
On magnetic rigidity, T×m	14 ÷ 40
Transfer efficiency, %	95
Transverse 95% emittances, hor/ver, *π·mm mrad*	3.0/8.0
Longitudinal root-mean-square momentum spread	$2 \cdot 10^{-4}$

The channel contains quadrupole lenses, bending and correcting magnets. To provide required stability of the beam parameters and stable long-term operation, new magnet power supply system was designed, constructed and put into operation during third commissioning run. The power supplies for the channel magnets are designed for currents from 600 A to 4000 A at relatively low voltage of 75-230 V.

The central system of electric power supply undergone an essential modernization since 2018. It is performed by Russian firms “Research and Production Enterprist LM Invertor”, “EPP-T”, “DCC engineering” and Polish firm “Frako Term”.

Commissioning of the upgraded channel, including vacuum, diagnostic and all the power supply systems is planned for fourth commissioning run.

1. The power supply system

The power supply system is designed to supply a precise DC current to the magnetic element (ME) to form the magneto-optical axis of the trajectory of charged particles in the building 205. The channel consists of dipole and quadrupole magnets designed to control the movement of charged particles through the transport channels. Existing ME are cooled with water and have a system of technological protections for overheating, disruption of the cooling system, control of the maximum current, etc. In normal mode, one power supply supplies ME only one of the channels. The electrical parameters of the magnetic elements are given in Table 2 below.

Table 2.

Parameters of magnetic elements

ME	I (A)	U (V)	R (Om)	L (H)	QuantityME
К-100	3500	75	0.021	0.010	7
К-200	3500	130	0.037	0.017	16
СП-94	635	212	0.334	0.870	5
СП-57	600	171	0.285	0.400	5
СП-12	1100	190	0.173	1.020	1
СП-12А	1700	215	0.126	0.600	6
СП-40	1100	220	0.200	1.710	3
СП-41	2500	300	0.120	1.800	1
МЛ-17	1280	160	0.125	0.027	1

The main features of the power supply system are high precision indicators for the accuracy of maintaining high current values (current from 600 to 4000 A) at relatively low

voltage values (from 75 to 230 V DC). The power supply system has redundancy on the supply voltage side and on the DC side.

The schematic diagram of the power supply system is shown in Fig. 2, it consists of the following elements:

- 6 kV network switchgear (SG) substation No. 15;
- power transformers 6/0.69kV;
- 0.69 kV network switchgear;
- high precision power supplies;
- switching cabinets;
- cable communications;
- automated control system.

Connection of the projected power supply system to the power grids of the JINR provides the voltage level of 6kV to five cells of outgoing lines of the renewed substation No. 15. The rated power of the power supply system is accepted in the amount of up to 5000 kVA.

The equipment of the power supply system is located in the existing premises No. 108 and No. 111, the experimental room along the wall and the new modular transformer building located next to the building 205.

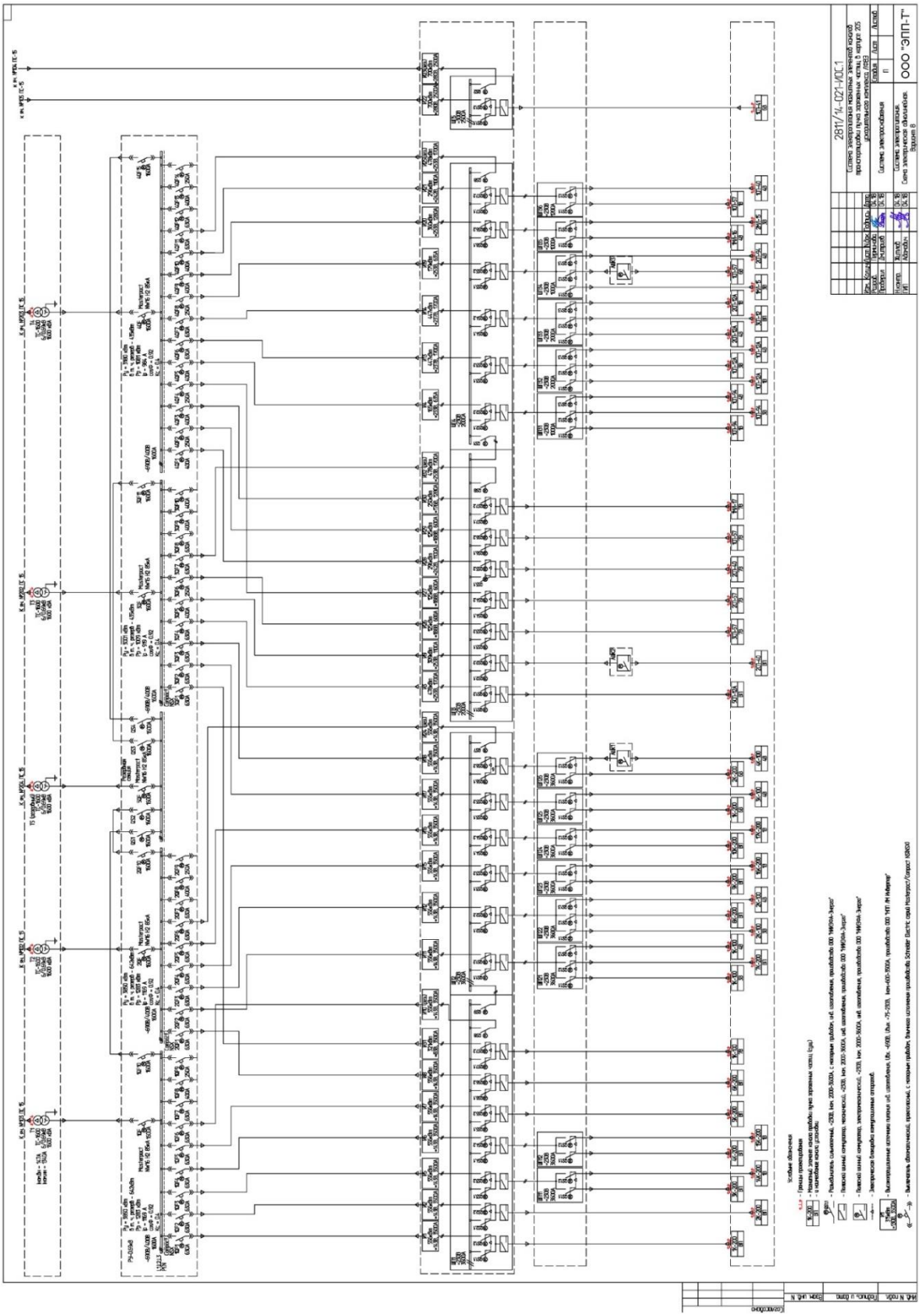

Fig. 2. A diagram of the power supply system for the beam output channel in building 205

1.1. 0.69 kV switchgear and power transformers

The main voltage of the power supply line of magnetic elements of the channel output beam of charged particles from the Nuclotron is adopted to 0.69 kV. Five dry power transformers TC3 6/0.69 kV of 1600kVA capacity powered from the reconstructed substation No. 15 are installed in a new modular building. Four power transformers are engaged during the normal operation of the power supply system of ME, the 5th transformer is used as a backup. Its inclusion is provided in the event of an accident at one of the TC3. The distribution of electricity at the level of 0.69 kV and the organization of the power supply system direct sources is carried out in switchgear SG-0.69 kV in room No. 108 and No. 111.

The distribution device at the voltage level is designed similarly to the power supply system of the beam output channel from the Nuclotron.

The mode of operation of the installation: 4 transformers workers, working on their own sections of tires, one transformer is in hot standby, and if necessary, feeds any of those four working section of busbar by switching its power to power from the fifth, reserved, section of busbar. Operation modes are controlled both in automatic and manual mode.

All switching devices are equipped with motor drives with the possibility of remote-control automated control system via RS485 channels.

1.2. Power supplies (PS)

The power supply system consists of 32 PS, of which 27 are working and 5 are in standby mode.

Main line of 30 PS is built on the principle of AC/DC converter and has a modular structure. The converter power of one module is 100-150 kW. The modules are connected in series or in parallel depending on the parameters of the ME. The converter unit as part of the module has a single circuitry and design for all types of sources. The parameters of the transformer and rectifier block are consistent with the parameters of the ME. The source is equipped with channels for receiving protections and locks from ME.

Two special power supplies (one main, the second backup) of the СП41 magnet are powered from 6kV network with substation №15 cells and each consists of 12 phase thyristor rectifiers and an active filter.

All sources are equipped with remote monitoring and control equipment included in the automated control system. The main technical parameters of power supplies are given in Table 3, weights and scales are shown in Table 4.

Table 3.

Main technical parameters of power supplies

№	Parameter name	parameter value	note
1.	Inputparameter		
1.1.	Supplyvoltage	three-phase voltage 690 (+/-10%) V	ForallPS
1.2.	The frequency of the mains	50 (+/- 2%) Hz	
1.3	Efficiency factor	notlower 0.92	
2.	Outputparameter		
2.1.	Output voltage	const,75-220 V	In accordance with the parameters of the ME
2.2.	Output current	635-4000 A	
2.3.	Rated power	140-600 кW	
2.4.	Operating mode	static	ForallPS
2.5.	The setting range of the output current	From 5% to the nominal value of PS	In accordance with the parameters of the ME
2.6.	The relative stability of the current	10^{-4}	ForallPS
2.7.	The resolution changes the output current	10^{-4}	
3.	The inductance of the load	0.01 – 0.87 H	determined by the parameters of the ME
4.	Load resistance	10…100 mOm	
5.	Cooling method	Forcedliquid	ForallPS
6.	Cooling liquid	Deionizedwater	
7.	Dimensions	1400×2000×800мм	For all PS except PS for ME type СП-94
		800×2000×800мм	PS for ME type СП-94

Table 4.

Weight and scale parameters of power supplies

ME	I (A)	U (V)	P (кW)	Dimensions (mm)	Weight(kg)
20К200	3500	130	455,0	1400×800×1800	800
20К100	3500	75	262,5	1400×800×1800	600
20К100*	4000	100	360,0	1400×800×1800	700
ВКМ	1600	200	320,0	1400×800×1800	700
СП-12А	1700	215	365,5	1400×800×1800	700
СП-94	635	212	134,6	800×800×1800	400

PS cabinets are placed in the room №108 and №111 in the close location to the SG-0.69kV.

1.3. Switching cabinets

Switching cabinets (SC) are intended for the organization of power backup of ME sources on DC circuits. Backup of power supply of ME is organized by means of transfer system of busbar which allows to make connection of ME to reserve power supplies. In SC

installation the disconnectors with nominal currents of 2000A and 4000A, with motor drives are provided.

Cabinets SC are designed for switching high-current DC circuits during absence of current. SC cabinets are connected to each other in rows and include busbars for rated current, which are connected to the reserve PS through a disconnector. The output circuits of the SC cabinets have in their design the technical possibility to change the polarity of the power terminals in the load cables.

Cabinets SC are equipped with locks that do not allow the simultaneous inclusion of two disconnectors. All SC are equipped with remote monitors and control included in automatic control system.

The main technical characteristics of the SC are given in Table 5.

Table 5.

Main technical characteristics of SC

№	Parameter name	parameter Value
1	voltage	DC, 250V
2	current	DC, 2000A, 4000A
3.	control voltag	AC, 50Hz, 220V
4.	Dimensions of cabinets	1400×600×2000 мм
5.	Degree of protection of cabinets	IP20

1.4. Cable communications

The power supply system of the ME is provided with busbars, power and control cables. For the organization of high-current circuits from power supplies to SC cabinets with rated current loads up to 2000A and 4000A the complete busbar bridges are used. Technical characteristics of the busbar and the choice of cable products is based on the rated current loads of power circuits, the length of the network and the possible method of laying. The total length of power cable lines is more than 8 km.

1.5. Automated control system

An automated process control system performs monitoring and control of power supply system's equipment. The automated control system consists of 7 cabinets of data acquisition and transmission devices, automated workstations of the operator and the engineering station.

Stand-alone cabinets are networked with the ability to transfer data to remote workstations via a server. Communication between power system objects and SCADA is organized via Modbus-RTU protocol, and via Ethernet between SCADA and operator. The automated control system provides information exchange with other levels of the hierarchy of management and operation of electrical networks. For the organization of non-stop power

supply the equipment of automated control system is equipped with uninterruptible power supplies.

1.6. Stages of the realization

The technical project for the power supply system was approved in 2019. In 2019, the building 208 was partially dismantled and the site was prepared for the construction of the new modular buildings substation No. 15 and Transformers (Fig. 3).

August 2018 *August 2019*

Fig. 3. Dismantling of the building 208

During 2020, construction work was finished and new modular buildings of substation 15 (PS 15) and Transformers were installed on that site. The equipment installation inside buildings was completed in 2021 (Fig. 4).

a) installation of Transformer building *b) Transformer and PS15 buildings*

c) installation of transformers

d) installation of PS15 cells

Fig. 4. Modular buildings PS15 and Transformers of the power supply system for magnetic elements of building 205

2. New Nuclotron beamlines for applied research

In the frame of ARIADNA (Applied Research Infrastructure for Advance Development at NICA fAcility) collaboration established in 2021, three new experimental stations are under construction:

- Iradiation Station of Components of Radioelectronic Apparatuses (ISCRA),
- Station for Investigations of Medico-Biological Objects (SIMBO),
- Station for High Energy Investigation in Nuclear Energetic (SHINE).

SIMBO and ISCRA stations are located in a special area including two beam channels that will be integrated into the existing Nuclotron-to-VP-1 extraction beam line (Fig. 5).

The SHINE station is located in the space between the old measurement pavilion and building 205 (Fig. 6).

Parameters of the extracted beams required for investigations at ISCRA and SIMBO stations are listed in Table 6.

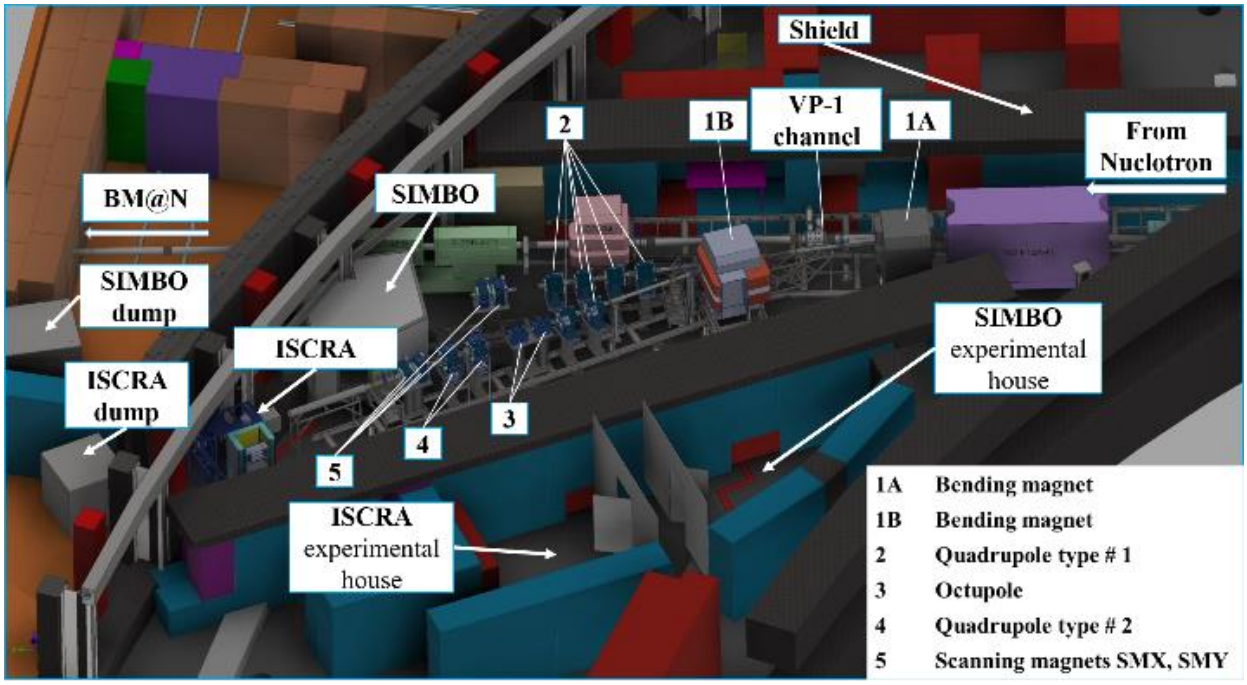

Fig. 5. Area 2 infrastructure layout.

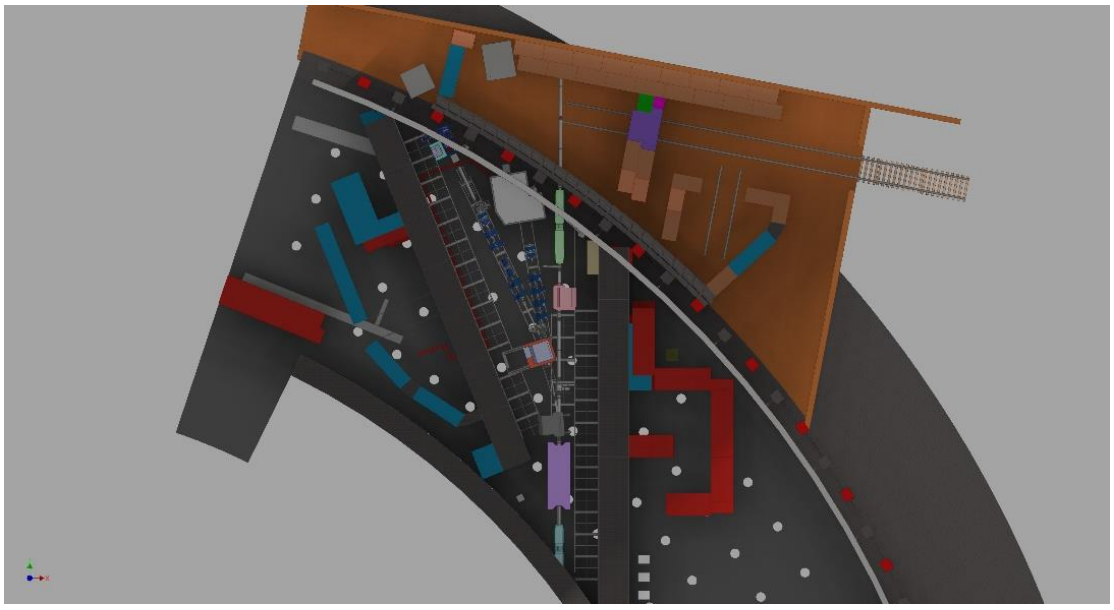

Fig. 6. Schetch of transfer line and SHINE station.

Table 6.

Ion beam parameters for applied research

Ion beam parameters		
Parameters	ISCRA	SIMBO
Ion types:	$^{12}C^{6+}$, $^{40}Ar^{18+}$, $^{56}Fe^{26+}$, $^{84}Kr^{36+}$, $^{131}Xe^{54+}$, $^{197}Au^{79}$	
Energy of ions, extracted from the Nuclotron, MeV/n	150-350	400-800
Energy spread at the Nuclotron exit, %	0,02	

Momentum spread (95%), less than, %	±0.1	
Pulse duration of extracted beam, sec	2-20	
Homogeneity of ion flow in time inside the pulse, %	99	
Intensity variation from pulse to pulse, %	10	
Vacuum, Torr	10^{-3}	
Extracted beam intensity, ion/impulse	3×10^4 - 10^8	$10^6 – 10^8$ (Xe, Kr, Fe, Ar) 10^7-$3\cdot10^9$($^{12}C^{6+}$)
Ion flux density, particles/(cm^2·s)	10^2-$3\cdot10^5$	103-105
Maximum fluency per irradiation session, ion/(cm^2)	2×10^7	10^7
Duration of exposure per session, min	10 - 20	1 - 5
Radiation dose, Gy		1 - 3
Normalized emittance, (95 %) $\varepsilon_x/\varepsilon_y\pi$·mm·mrad	4.7/12.5 (working) 15.7/23.5(maximum)	
Beam emittance at the entrance to the stand at maximum energy, (95 %) $\varepsilon_x/\varepsilon_y\pi$·mm·mrad	5/13.3 (working) 16.6/24.9(maximum)	3/8 (working) 10/15(maximum)
Target irradiation area without scanning, mm	20 × 20 (10 %)	∅10 (5 %)
Maximal irradiation area in scanning mode, mm	200 × 200	100 × 100
Homogeneity of ion flow at the maximal irradiation area	±15%	±10%
Beam full width at half maximum on the target, mm	30 - 57 (73 mm for Gaussian beam)	25 - 35

2.1. Magnetic system of the new beam lines

The old part of the Nuclotron channel consists of the septum, the Lambertson magnet, the triplet of quadrupole lenses, the duplet of lenses, and the vertical deflection dipole magnet.

In addition to the existing dipole magnets that serve to direct the beam from the Nuclotron to the channels, the ISCRA and SIMBO channels will be equipped with new scanning magnets, two new families of quadrupoles and new octupole magnets (see Table 7). The scanning vertical and horizontal magnets serve to from a uniform dose distribution with a large chip target area of 200×200 mm and radiobiological target area of 100×100 mm.

Table 7.

Main requirements for new magnets for the ISCRA and SIMBO channels

	Scanning magnet	Quadrupole		octupole
Parameter	SMX/SMY	Type 1	Type 2	
# magnets	2+2	6	2	2
Gap/bore Ø (mm)	140	108	160	105

Field/Gradient (T, T/m, T/m^3)	±0.8	0.6-5.4	0.2-1.4	1098
L_{eff} (mm)	356±4	492±2	480±2	505±3
Good Field Region (mm)	H×V 60 x 60	Ø 100	Ø 128	Ø 90
Rel. integrated field error ×10^{-3}	< ±5	< ±5	< ±5	< ±5
Operating mode	Scanning f=0.5-3 Hz	DC	DC	DC

2.2. Beam diagnostics

Three types of detectors will be used for beam diagnostics in the channels in the Measurement Hall:

- an offline multiwire proportional ionization chamber (1 pcs. 100×100 mm and 2 pcs. 75×75 mm),
- scintillating fiber detector (1 pcs. 100×100 mm and 2 pcs. 75×75 mm)
- two systems for online diagnostics (4 scintillating fiber based detectors 20×20 mm).

The offline systems duplicate each other to get more reliable results. Beam diagnostics in each of the channels will be in conjunction with the beam diagnostics at the stations.

The beam diagnostics will operate in the “tuning” and “irradiation” modes. All detectors are placed on stepper motors that transversely move and withdraw detectors from the beam area. The diagnostics equipment is designed to measure and control such beam characteristics as ion flux density, ion fluence, ion beam linear energy transfer (LET), mean energy, beam profiles, and absorbed dose.

2.3. The ISCRA station

The ions $^{40}Ar^{18+}$, $^{131}Xe^{54+}$ and $^{197}Au^{79+}$ at the energy of 150-350 MeV/u are decelerated in a degrader and the capsule covered microchip to the energy of 5-10 MeV/u corresponding to the Bragg peak. The linear energy transfer (LET) is 60-70 MeV·cm^2/mg for $^{197}Au^{79}$ ions in the Si chip for this energy.

The ISCRA beam diagnostics will operate in the “tuning” and “irradiation” modes. The diagnostics provides measurements of the following parameters at the chip irradiation:

- the ion beam profiles,
- the primary ion fluency,
- the primary ion density flux,
- the secondary particle density flux and the radiation dose.

The tuning diagnostics (Table 8) consists of ionization chambers with different working areas of 10 × 10 mm, 80 × 80mm and 250 × 250 mm and scintillation detector with working area of 80 × 80 mm. The online diagnostics in irradiation modes involves three scintillation detectors and one silicon detector installed at a large aperture to measure and control peripheral ion characteristics.

Table 8.

ISCRA tuning diagnostics

Parameter	Value
Intensity, fluence, profile and flow density measurement in non-scanning mode	
Ionization chamber, scintillation detector	
Input port diameter, mm	90
Working field, mm	80 × 80
Ion energy range, MeV/n	10 - 500
Accuracy of ion flux measurement	±10%
The beam time structure measurement, polling rate, Hz	20
Fluence measurement	Yes
Space resolution, mm	2-3
Accuracy of beam inhomogeneity measurements	±10%
Ionization chamber for scanning regime	
Working area, mm	250 × 250
Ion energy range, MeV/n	10 - 500
Accuracy of ion flux measurement	±10%
Fluence measurement	Yes
Accuracy of beam center gravity definition, mm	3
Accuracy of dispersion definition, mm	5
Accuracy of beam inhomogeneity measurements, mm	±15%

The conceptual project of chip irradiation station ISCRA was prepared by ITEP-JINR collaboration in 2018. The equipment of the station, constructed since autumn 2019 by the JINR-ITEP collaboration, is being assembled now (Fig. 7, 8). First beam run is planned for 2023.

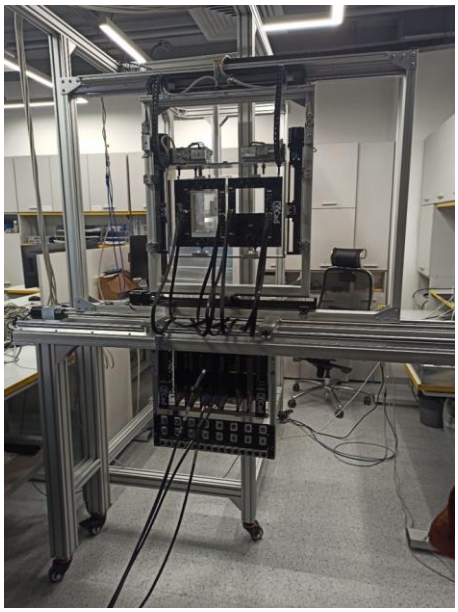

Fig. 7. Diagnostics of the ISCRA station.

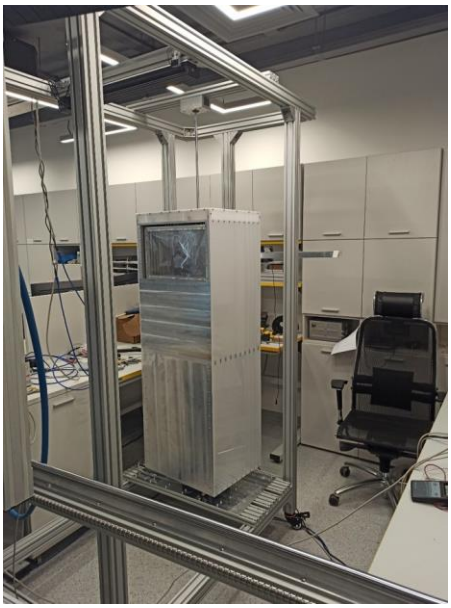

a) *b)*

Fig. 8. Equipment of the ISCRA station: a) electronic equipment in radiation shielding, b) beam degrader.

2.4. The SIMBO station

Heavy ions extracted from the Nuclotron at the energy of 0.4-0.8 GeV/u are suitable for modelling of biological action of cosmic space radiation. They will be used for producing a typical dose of one Gy required for radiobiological researches. The equipment of the radiobiological SIMBO station (Fig. 9, 10*)* permits ion irradiation of biological samples and animals like rats and monkeys.

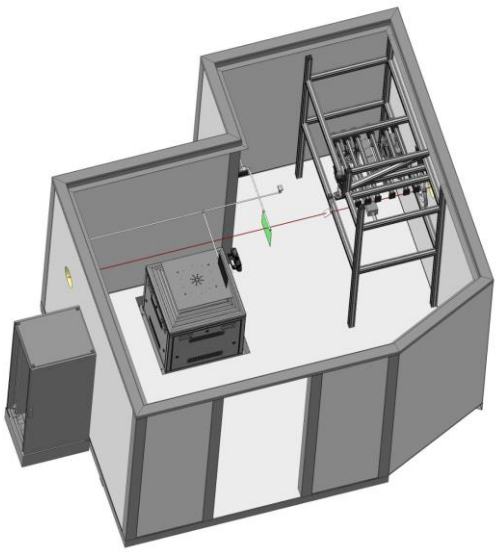

a) *b)*

Fig. 9. a) 3D-view of SIMBO station, b) SIMBO beam diagnostic equipment.

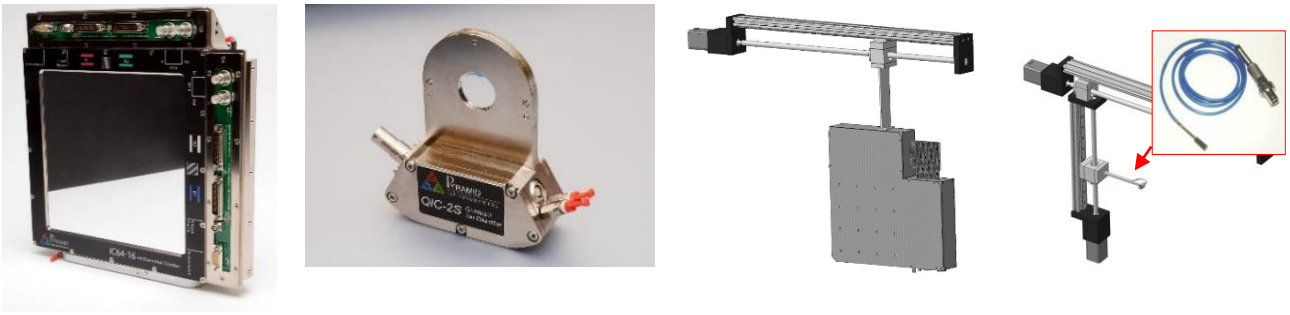

a) *b)* *c)* *d)*

Fig. 10. SIMBO beam diagnostic equipment: a) Ionization chamber b) Dose ionization chamber, c) Scintillating fiber detector, d) Diamond semiconductor detector.

A uniform dose distribution will be formed in the target with the maximal size of 100×100 mm and depth of 100 mm. Scanning magnets are used for this dose formation. The diagnostic system is used for measuring of the ion flux, the horizontal and vertical profiles and controlling the beam position relative to the target optical axes, dose space distribution and received dose. The tuning diagnostics consists of ionization chambers and scintillation detectors. The special chair for monkey 3D positioning (Fig. 11) with accuracy better than 1mm was developed. The microclimate and special temperature will be prepared inside of the SIMBO irradiation cabin.

Fig. 11. SIMBO special 3D chair and its control system.

Conceptual project of the SIMBO station was prepared by ITEP-JINR collaboration in 2018. The construction of SIMBO was started in Summer 2020 by firm “Vacuum systems and technologies” (Belgorod). Installation of equipment has started in March 2022.

2.5. The SHINE station

The SHINE station is under development for obtaining new nuclear physics data on interaction of relativistic (0.3-4.5 GeV/n) beams of protons, deuterons and light ion with intensities of 10^5-10^{10} p/s for prototype of ADS targets and fuel assemblies for verification of physical models and codes in design of ADS facilities and neutron sources.

The station is located in the space between the old measurement pavilion and building 205. It will be applicable for irradiation of large compound targets. An air gap of 3-3.5 m in the vacuum beam line is closed by two gates designated for installation of the diagnostic vacuum box in front of the experimental irradiation zone. This diagnostic box with detectors for non-destructive measurements of the time and space structure of the beam will be applied to provide reliable determination of beam parameters both for experiments in building 205 and for the SHINE station for irradiation of big compound targets. The spacing between the buildings (about 9 m) is sufficient to create reliable biological shielding both for irradiation of big targets and subsequent storage of irradiated samples. The station will include a remotely controlled movable platform for positioning of heavy targets/shields and 3m tube for connection to the vacuum beam line.